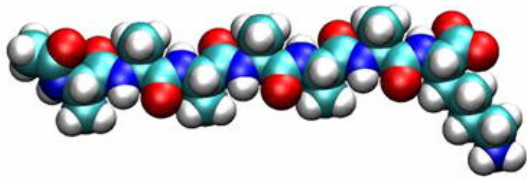
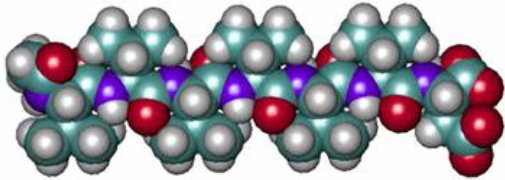


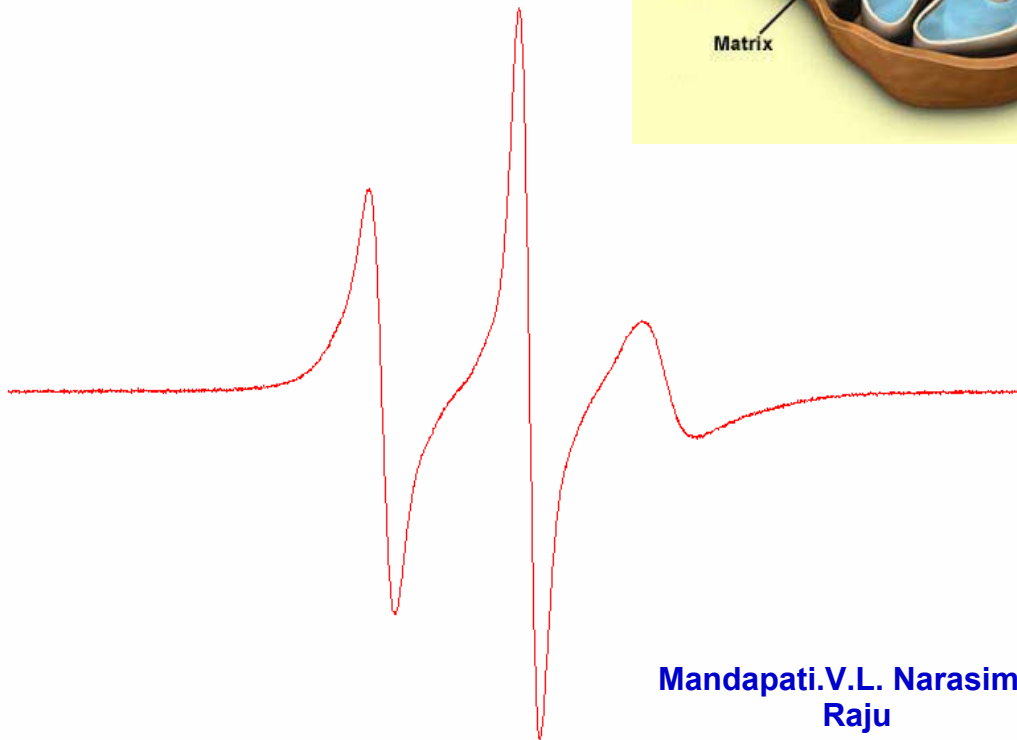
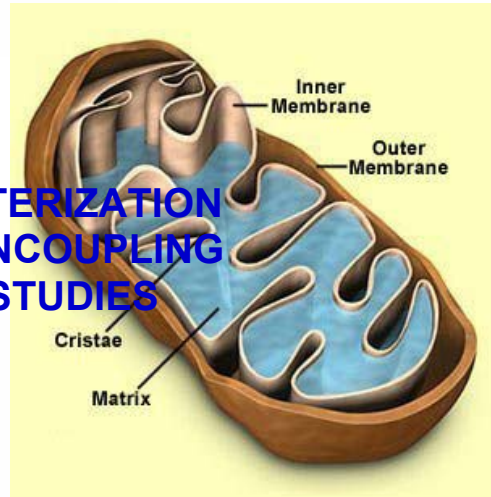
**Hydrophobic Tail**



**Hydrophilic Head**



**FUNCTIONAL CHARACTERIZATION  
OF MITOCHONDRIAL UNCOUPLING  
PROTEIN 2 BY EPR STUDIES**



**Mandapati.V.L. Narasimha  
Raju**

**FUNCTIONAL CHARACTERIZATION OF  
MITOCHONDRIAL UNCOUPLING PROTEIN 2  
BY EPR STUDIES**

Vom Fachbereich Chemie  
der Technischen Universität Kaiserslautern  
zur Verleihung des akademischen Grades  
“Doktor der Naturwissenschaften”  
genehmigte Dissertation

Betreuer: **Prof. Dr. Wolfgang. E.Trommer**

Vorgelegt von  
**Mandapati V.L.Narasimha Raju**  
Kaiserslautern 2006

Datum der wissenschaftlichen Aussprache: 15.08.2006

Promotionskommission:

Vorsitzender: **Prof. Dr. Dr. Dieter Schrenk**

1. Berichterstatter: **Prof. Dr. W.E.Trommer**
2. Berichterstatter: **Dr. Petr Ježek**

Examining Board:

Board Chairman: **Prof. Dr. Dr. Dieter Schrenk**

1. Reviewer: **Prof. Dr. W.E.Trommer**
2. Reviewer: **Dr. Petr Ježek**

## **Table of Contents**

<b>Introduction</b>	<b>1</b>
Membrane proteins	2
Uncoupling protein	4
EPR spectroscopy	8
Spin labels	14
<b>Objective</b>	<b>18</b>
<b>Abbreviations</b>	<b>21</b>
<b>Methods and Materials</b>	<b>23</b>
<b>Results and Discussions</b>	<b>34</b>
Spin-labelled fatty acids as substrate	35
Competition with natural fatty acids	38
Alkyl sulfonates as competitors	43
Role of UCP2 in ROS production	48
Effect of purine nucleotides on UCP2	50
<b>Summary</b>	<b>55</b>
<b>Zusammenfassung</b>	<b>57</b>
<b>References</b>	<b>59</b>

## INTRODUCTION

One of the main targets of current biochemical research is a molecular understanding of the function of biological membranes, one of the most important structures in the living systems. Membranes form a boundary between many of the quasi-independent systems which biochemists try to isolate and study. Cells, for example, are bounded by membranes, nutrients and waste products pass through, and the sites at which cells can be recognized by other cells and by small molecules are situated on the cell membrane.

The cell organelles of eukaryotic cells, - the nuclei, mitochondria, endoplasmic reticulum and others – are bounded by membranes, each with its characteristic function. A cell which is divided into compartments by membranes is able to control its activity in a most sophisticated way. It becomes possible for the different compartments to contain different concentrations of metabolites. The asymmetric distribution of small molecules that can result allows the development of energy-conservation devices such as mitochondria and chloroplasts. Processes within the individual compartments can be controlled separately, leading to a greater efficiency in energy production and utilisation. Membranes also provide an apolar matrix within which the synthesis of water-insoluble compounds such as cholesterol can take place.

The basic components of membranes are well known. Apart from the rigid cell wall structures in plants and many micro-organisms, the main membrane components are protein and lipid. Many types of lipid molecules are known, and they all have one basic chemical property in common: they are all soluble in organic solvent mixtures (commonly a mixture of chloroform and methanol is used) and insoluble in water. This water immiscibility is due to the high hydrocarbon content of all lipid molecules, and means that when suitably organised they are capable of serving as a boundary between aqueous regions. Two of the most commonly studied lipids in membranes are the phosphatidyl cholines, members of the class of phospholipids, and the sterol cholesterol. The high hydrocarbon content of these molecules is immediately apparent: one would not expect them to be soluble in water. When we examine the structure of phosphatidyl choline more closely, we can distinguish two main features. Firstly the long hydro-carbon chains, in addition, a polar group, the phosphate ester of choline, which is attached to C-3 of the glycerol. We would expect this polar group to prefer

an aqueous environment. The forces involved in this interaction are clearly those of polar groups being stabilised in a polar environment, and also a strong hydrophobic interaction between the adjacent hydrocarbon chains of the phospholipids. In many ways the phospholipid molecules, in their orientation at an aqueous surface, are behaving like detergent molecules. Detergents are also amphipathic (contain both a polar and an apolar group) and can form micelles. Micelles are short lived aggregates of amphipathic molecules.

One of the most characteristic properties of a liquid is its fluidity, and this is thought to be a very important property of biological membranes. Too rigid membranes may prevent the diffusion of small molecules across the bilayer or inhibit membrane-bound proteins. A cell with too fluid a membrane may be over-fragile and unable to maintain its internal environment satisfactorily.

### **Membrane proteins in general -**

Membranes are selectively permeable barriers which compartmentalise, and thereby exert considerable control over, cellular metabolism. They provide the support and working environment for a great variety of enzymes, receptors and antigens, each of which interact with soluble material in the aqueous milieu either at one or both surfaces of the membrane. Sites may also be provided through which the membrane can interact with cytoskeletal elements, as in cell movement or during secretion. All of these functions are achieved by a hydrated structure that is essentially constructed of a bilayer of lipid molecules with which various types of proteins and glyco-proteins are associated: some penetrate through the lipid bilayer, some are inserted into it only from one side, whilst others are associated with the membrane in a more superficial manner which does not involve direct interaction with the inner parts of the lipid bilayer. Most membrane functions are the functions of the membrane proteins and glycoproteins, and the relative variety and abundance of the protein species found in any individual membrane are to some extent a reflection of the diversity and intensity of its biological activities.

The proportion of the dried weight of various membrane preparations which is protein varies within the range of 20 to 75%. At the lower extreme is nerve myelin which exhibits only a few relatively weak enzyme activities: its major function appears to be as an electrical insulator. An example of the membrane which has about three-quarters of their dried weight

as protein is the inner mitochondrial membrane which has a highly complex mixture of components involved in electron transport, ATP synthesis, solute transport and membrane potential (proton motive force). The interpretation in structural terms of this variability in protein content between different membrane proteins is not straight forward, in that it must take account of the fact that some proteins are superficially attached at the hydrated surfaces of membranes (extrinsic or peripheral proteins) whilst others include regions which are inserted to a significant extent into the apolar interior of the membrane (intrinsic or integral proteins).

**Uncoupling proteins –**

Uncoupling proteins (UCPs) belong to the mitochondrial anion carrier family. These proteins mediate a regulated discharge of the proton gradient that is generated by the respiratory chain. UCP2 was discovered in 1997, revealed by screening the human and mouse expressed sequence tag (EST) libraries (Fleury et al.1997; Gimeno et al.1997). Its mRNA has been identified in several tissues as heart, kidney, lung, placenta, white fat and tissues of the immune system. Human UCP2 shows 59% homology with the well-known UCP1 of brown adipose tissue (BAT) mitochondria, also called thermogenin (Fleury et al.1997; Gimeno et al.1997). It was found that UCP1 allows protons to re-enter into the mitochondrial matrix, uncoupling the electron transport from oxidative phosphorylation (synthesis of ATP). The result is heat production (Klingenberg 1990; Nicholls 1979).

It is accepted that BAT and UCP1 are involved in the so-called non-shivering thermogenesis that is the phenomenon of absence of shivering in newborn, cold acclimated and hibernating mammals (Nedergaard and Cannon 1992). When new UCP isoforms (UCP2 to UCP5) were identified in humans or in rodents, mitochondria were recognized not only as simple energy generators, but also as organelles regulating various physiological phenomena (Ježek et al.2004).

The physiological functions of UCP2 are still unknown. It may play a role in muscle non-shivering thermogenesis, regulation of body weight and in protection against formation of reactive oxygen species (ROS) (Nedergaard and Cannon 2003). ROS are significantly produced in mitochondria (Turrens 1997; Brookes et al. 2004; Boveris and Change 1973; St. Pierre et al. 2002; Staniek et al. 2002; Kwong and Sohal 1998). Any slight increase of the  $H^+$  back flux to the matrix, which diminishes the proton motive force  $\Delta p$  (electrochemical  $H^+$  gradient), has been shown to decrease ROS generation (Brookes et al. 2004); this is a well documented phenomenon from experiments using artificial uncouplers (Korshunov et al. 1998; Skulachev 1998). The function of UCP2 as an uncoupling agent could therefore be to keep the membrane potential sufficiently low for ROS production to be minimized (Nedergaard and Cannon 2003). Consequently great pharmacological potential is expected in revealing biochemical and hormonal regulation of UCP2. Recent work has shown that the UCP homologues are activated by a superoxide dependent mechanism. This observation led to the suggestion of a feedback mechanism which controls the production of reactive oxygen

species; however, the importance of the UCP homologues in cellular antioxidant defense is not clear at this point. Although the physiological functions of UCP2 and UCP3 remain uncertain, it has been shown that UCP2, by virtue of its proton-leak activity, has an important role in the patho-physiology of type-2 diabetes. In particular, hyperglycaemia causes a pathological, superoxide dependent activation of UCP2 in pancreatic islets, which, in turn, causes loss of glucose-stimulated insulin secretion.

Further work is required to elucidate the physiological roles and regulation of UCP2 and UCP3, and to understand, at a molecular level, how they mediate proton leak. This will have implications for many pathologies and diseases: for example, targeted inhibition of UCP2 should be a useful tool in the treatment of pancreatic- $\beta$ -cell dysfunction and type-2 diabetes.

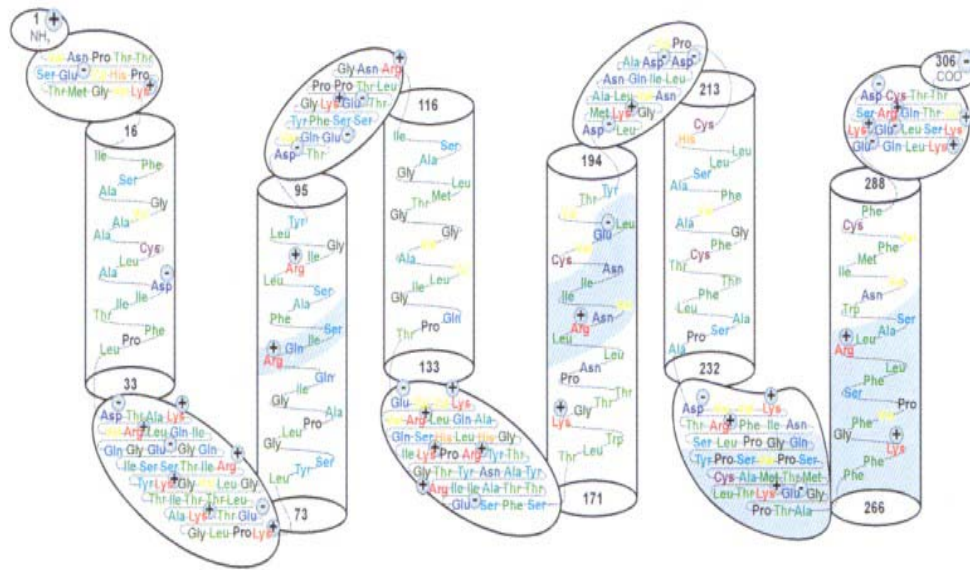
### **Structure and mechanism –**

UCPs have a characteristic molecular mass of 31-34 KDa and a tripartite structure in which a region of around 100 residues is repeated three times; each repeat codes for two transmembrane segments and a long hydrophilic loop. The three internal repeats are homologous to each other and form six membrane-spanning quasi  $\alpha$ -helices (Fig.1.1).

In UCPs the C- and N-ends are located on the cytosolic side of the mitochondrial inner membrane, resulting in four cytosolic and three matrix segments ( Klingenberg 1990; Moualij *et al.* 1997). Because of similar structure to UCP1, there is substantial evidence to assume an identical molecular mechanism of uncoupling for UCP2, even if the question is still controversial.

UCP1 catalyses the flip-flop transport of the anionic fatty acid (FA) head group from one side of the membrane to the other (Fig.1.2) (Garlid *et al.* 1996). It enables FA to behave as cycling protonophores, dissipating  $H^+$  gradient and preventing ATP synthesis on  $F_0F_1$ -ATPase (Ježek and Garlid 1998).

### Intermembrane space



### Matrix

**Fig. 1.1:** Mammalian (rat) uncoupling protein structure – a model for trans-membrane spanning as suggested by Klingenberg. The shadowed areas are the loci interacting with purine nucleotide di- and triphosphates.

Normally, despite high electrical gradient *in vivo*, there is no significant flux of FA anion because the bilayer energy barrier is high. The mechanism of uncoupling for UCP1 has been demonstrated to be the following: the FA anion from the matrix bilayer leaflet diffuses laterally to reach the protein and interacts with the internal binding site that lowers the energy barrier; the electric field drives the anionic head group to the energy well. The hydrophobic tail moves to the other side of the membrane principally by the same mechanism that occurs as the flip-flop of the protonated fatty acid; protonation is now insured by the protein. After the release from the internal binding site, protonation of the FA at the opposite site of the membrane proceeds and neutral FA can rapidly flip-flop back (Garlid *et al.* 1996).

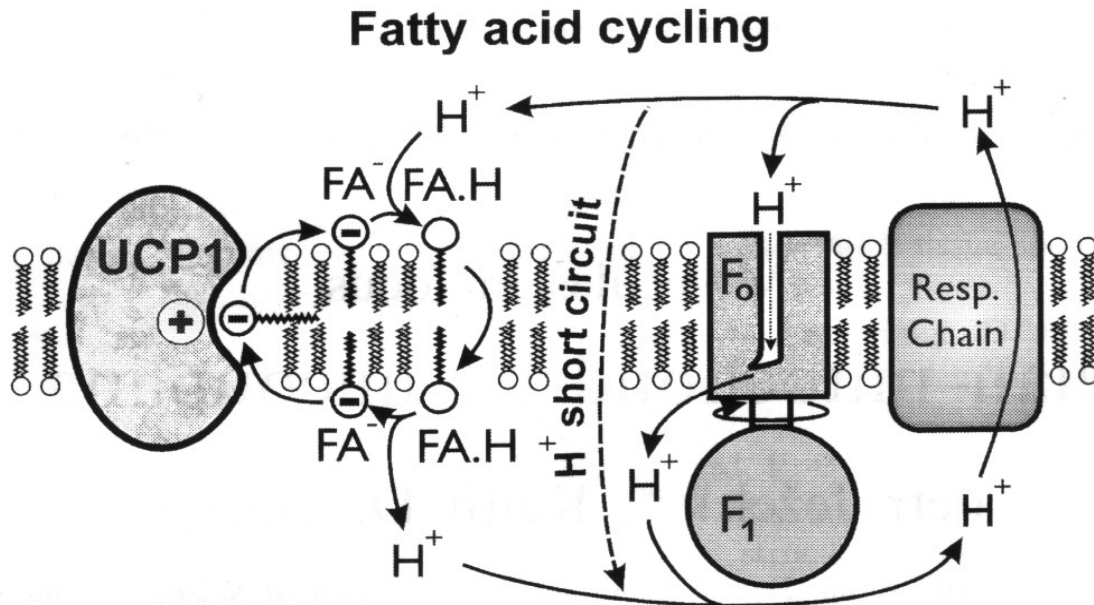


**Fig. 1.2:** *Fatty acid cycling*

The net transport of protons is regulated in several ways. Adenine nucleotides strongly inhibit transport, whereas FAs serve as activators. The regulatory purine nucleotide (PN) binding site is purely allosteric (Ježek and Garlid 1998). The receptor site has a high affinity to PN di- and triphosphates and a low affinity to PN monophosphates; pyrimidine nucleotides neither bind to UCP1 nor inhibit transport (Klingenberg *et al.* 1990; Winkler *et al.* 1997). Purine nucleotide binding and inhibition decrease with increasing pH. The inhibited conformation is achieved only when the  $\alpha$ -phosphate binds to R276. This induces conformational changes occluding the internal fatty acid binding site, causing inhibition of transport (Garlid *et al.* 1996; Modriansky *et al.* 1997).

The transport pathway is predicted to possess an internal weak binding site near the middle point of the membrane and to lie on an outside surface of one of the transmembrane helices at the protein-lipid interface. It is usually assumed that UCP2 have identical molecular properties as UCP1. Fatty acids were found to be essential also for UCP2 induced uncoupling and ATP and GDP to be inhibitors of the supposed mechanism. EPR spectroscopy of spin-

labelled fatty acids was used to investigate the putative FA binding site on UCP2 and the existence of a distinct nucleotide-binding site.

The alignment of the amino acid sequences of UCP1, UCP2 and UCP3 shows that these proteins are significantly similar (Fig 1.3 and Table 1.1). These proteins exhibit a triplicated structure and a signature motif that is also present in other mitochondrial carriers. A similar organization was observed in plant UCPs. No N-terminal mitochondrial cleavable targeting sequence is present in UCP1, and sequence comparison suggests that the other UCPs are similar. Computerized analysis of the secondary structure of the UCPs predicted the existence of six transmembrane domains linked by polar loops (Aquila, H *et al.* 1985, Bouillaud, F *et al.* 1986). Several antigenic sites in rat UCP1 were identified in an approach to study the topology of protein in mitoplasts and sonicated mitoplasts. These studies validated the predicted secondary structure of UCP1. Considering the above studies and the present data explained in our study, it can be proposed that the different UCPs share the same type of folding in the membrane.

### **EPR spectroscopy -**

**Electron Paramagnetic Resonance (EPR)**, often called **Electron Spin Resonance (ESR)**, is used for the branch of spectroscopy that studies paramagnetic molecules, that is molecules with unpaired electrons. Biologically important paramagnetic species include free radicals and many transition elements. In addition there is substantial and rapidly growing use of synthetic stable free radicals (eg: spin labels) to obtain information on a wide variety of complex biochemical systems such as macromolecules and membranes.

### **Theory**

An isolated electron, all alone in space without any outside forces, has an intrinsic angular momentum (impulse) called spin. In general the spin  $s$  is limited to  $2s+1$  discrete states. For a single unpaired electron  $s = \frac{1}{2}$ , so there are only two possible spin states, which we can consider as spin in opposite direction and that have the same energy in the absence of a magnetic field. The value that  $s$  takes along a specified direction ( $z$  axis) is then  $+1/2$  or  $-1/2$ . (The two spin states of the electron are often labelled by their values of  $m_s$ ). Because of

its charge and angular momentum the electron generates a magnetic field, so it acts like a little bar magnet or magnetic dipole with a magnetic moment  $\mu$  (Fig.1.3).



**Fig. 1.3:** Free, unpaired electron in space: electron spin, magnetic moment

### **Zeeman effect**

If the unpaired electron is placed in an external magnetic field  $B_0$ , its magnetic moment interacts with the magnetic field, producing two energy levels, otherwise degenerated. This effect is called Zeeman effect. The energy of interaction is equal to the product of the magnetic field and the projection of the magnetic moment  $\mu$  along the direction of the magnetic field, which is generally defined to be  $z$ :

$$E = \mu_z B_0$$

However, unlike the magnetic moment of the bar magnet, the quantum nature of the electron restricts its magnetic moment to two possible orientations, parallel or antiparallel to the field. Hence it will have a state of lowest energy when its moment is aligned with the magnetic field and a state of highest energy when the moment is aligned against the magnetic field (Fig.1.4).

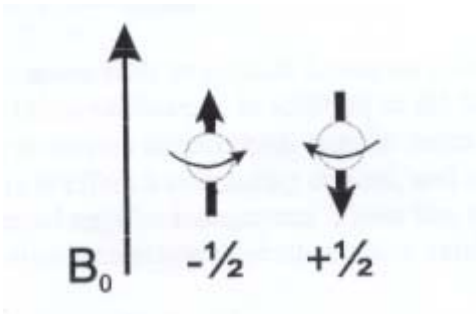


**Fig. 1.4:** Minimum and maximum energy orientations of  $\mu$  with respect to the magnetic field

$B_0$ .

The magnetic moment  $\mu_z$  of an electron is proportional to its spin through the relationship:

$$\mu_z = g_e \beta m_s$$

where  $\beta$  is a conversion constant called ‘‘Bohr magneton’’ and  $g_e$  is the spectroscopic  $g$  factor of free electron called Landé factor and equals to 2.0023. Therefore the energy in the magnetic field is:

$$E = g_e \beta B_0 m_s$$

Consequently in a magnetic field two energy levels exist:

$$E = +1/2 g_e \beta B_0 \quad \text{and}$$

$$E = -1/2 g_e \beta B_0$$

separated in energy by an amount  $g_e \beta B_0$  (Fig.1.5). From this equation derives that in absence of magnetic field there is only one energy level and that the energy difference depends linearly on the magnetic field.

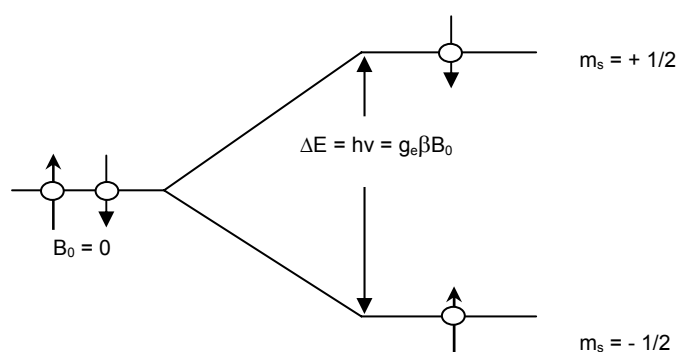


**Fig. 1.5:** Energy levels of an unpaired electron in a magnetic field.

Electromagnetic radiation of frequency  $\nu$  such that  $h\nu = g_e \beta B_0$  can be used to induce transitions between these levels (Fig.1.6). At the magnetic fields usually used for ESR experiments, the separation of the levels is such that this frequency lies in the microwave region of the electromagnetic spectrum.

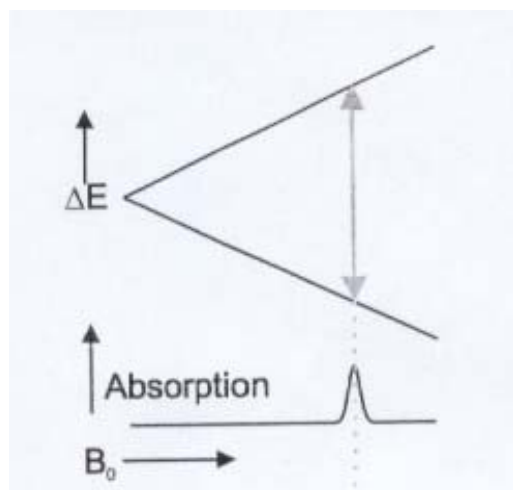


**Fig. 1.6:** Variation of the spin state energies as a function of the applied magnetic field  $B_0$ .

### Hyperfine splitting

The basic ESR resonance line from the electron can be split into two or more hyperfine lines, if the unpaired electron spends significant time close to nuclei with magnetic moments, so that there can be magnetic interaction between magnetic nuclei and the electron (Fig.1.7). Nuclei have magnetic moments if they have net nuclear spin ( $I \neq 0$ ). The splitting of the energy levels of the unpaired electrons is due to the small magnetic field  $B_1$  associated with nuclei that have magnetic moments. This magnetic field opposes or adds to the magnetic field from the laboratory depending on the alignment of the moment of the nucleus. When  $B_1$  adds to the magnet field, we need less magnetic field from our laboratory magnet and therefore  $B_1$  lowers the field of resonance. The opposite is true when  $B_1$  opposes the laboratory field.

In biological systems, nuclei with magnetic moments include nitrogen  $^{14}\text{N}$  ( $I=1$ ), hydrogen  $^1\text{H}$  ( $I=1/2$ ), deuterium  $^2\text{H}$  ( $I=1$ ), and carbon  $^{13}\text{C}$  ( $I=1/2$ ), as well as nuclei of some transition metals. Magnetic moments of nuclei are only about 1/600 as large as that of the electron and may have several possible values instead of only two. The number of possible values of magnetic moments is  $2I+1$ , where  $I$  is the spin of the nucleus. So the magnetic

interaction between magnetic nuclei and the electron produces a splitting of the basic resonance line into  $2I+1$  number of hyperfine components.

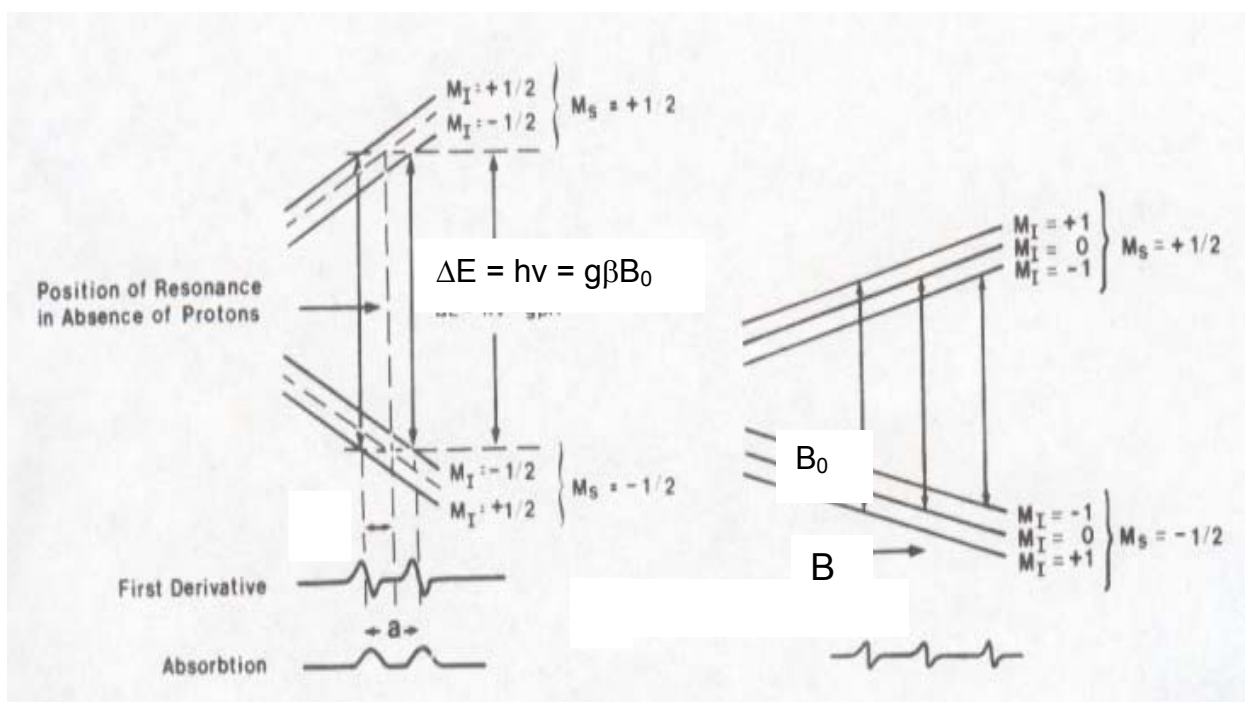


**Fig. 1.7:** Simple modifications of ESR lines (hyperfine splitting) due to interaction of the unpaired electron with particular nuclei. a) Interaction with a proton  $I=1/2$ ; possible spin states  $m_I = +1/2; -1/2$ . b) Interaction with nitrogen  $I = 1$ ;  $m_I = 1, 0, -1$ .

The effect of hyperfine interaction is to add a term to the energy expression for an EPR transition:

$$\Delta E = hv = g\beta B_0 + hA m_I$$

where  $A$  is called the hyperfine coupling constant (measured in  $\text{cm}^{-1}$  or MHz) and  $m_I$  is one of the  $2I+1$  projections of the nuclear spin.

Hyperfine splittings are dependent on the orientation of the molecules in the magnetic field; in particular their magnitude depends on the angle between the axis of the molecule and the applied magnetic field. When the molecule rotates sufficiently rapidly, anisotropic components are averaged out, but when the motion is slower, hyperfine lines begin to broaden (Fig.1.8). This rotation depends both on the size of the molecule and on the viscosity of the solution.

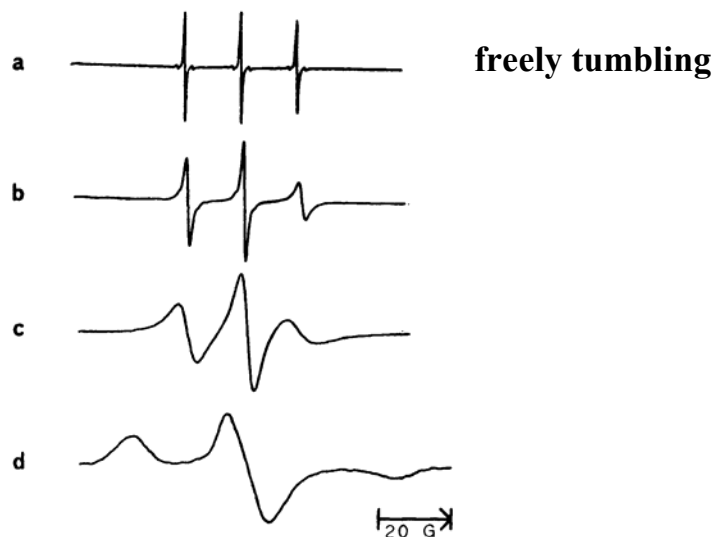


**Fig.1.8:** Normalized EPR spectra of a spin label with increasing viscosity/motional restriction.

### The g-factor

In analogy with orbital angular momentum, for which the magnetic angular moment along  $z$  axis is  $\mu_L = \beta m_L$ , the magnetic moment of the electron  $\mu_z$  should be  $\beta m_s$ . However, detailed interpretation of early experimental results showed that the actual magnetic moment appeared to be twice this. More recent experiments have shown that it is more correct to write:

$$\mu_z = g_e \beta m_s$$

where  $g_e$  is the g-value of the free electron (2.0023).

The g-factor is defined mathematically as  $g = h\nu/\beta B$ . For symmetrical ESR spectra, the g-value can be obtained from the field position of the centre of the resonance. For most free radicals the g-value is close to the value for the free electron. However, small deviations from the free electron value that are found are quite significant. In particular, shifts occur for unpaired electrons located near nuclei with low-lying excited states (e.g. oxygen, sulphur and especially transition elements); coupling of the spin of the electron to the orbital motion can occur, and as a result, the g-value shifts. Such shifts can greatly assist in the identification of unpaired electron species in complex biological systems.

Just as the hyperfine interaction, the  $g$ -value of a paramagnetic molecule oriented in space depends upon the direction along which it is measured; it is anisotropic. Again, when the molecules undergo very rapid rotation, the isotropic components of the  $g$ -value average out, but with slower motion these components affect the spectrum (Fig.1.8).

### Spin labels

A spin label is a paramagnetic group, usually a nitroxide stable free radical that is introduced to make the experimental system accessible to be studied by ESR. Spin labels can provide information on motion, both the motion of the spin label itself and of the molecule or molecular system to which it is bound, and also provide information on the chemical nature of the environment of the site at which the label is bound.

The major structural elements of a nitroxide spin label are the nitrogen-oxygen bond, which contains the unpaired electron, necessary to produce an ESR signal, and the steric hindrance of the NO group by bulky groups on the carbon atoms attached to the nitrogen. In the usual convention, the  $z$  axis extends along the nitrogen's  $p$  orbital, in which occurs much of the spin density, the  $x$  direction is along the N-O bond, and  $y$  is mutually perpendicular to  $x$  and  $z$  (Fig 1.9).

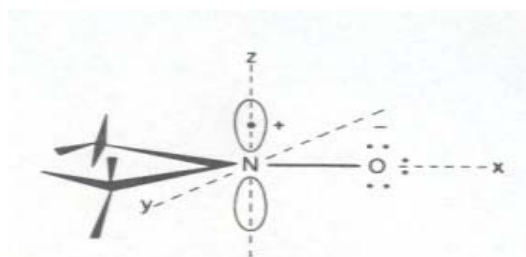


**Fig. 1.9:** Chemical structure of a nitroxide spin label.

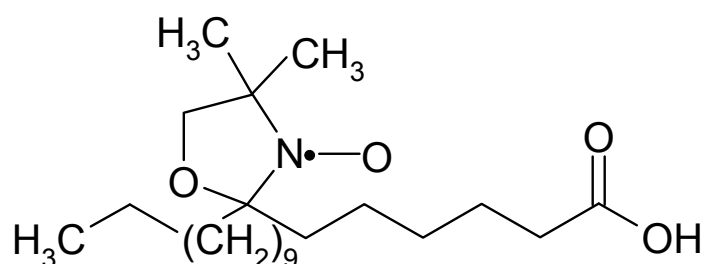
The ESR spectrum of a nitroxide spin label is split into three principal lines because of interactions with the nitrogen nucleus (which has spin of 1). The magnitude of this hyperfine splitting depends on the orientation of the nitroxide free radical in relationship to the applied magnetic field. It is this fact combined with the orientation dependency of the  $g$ -values that makes nitroxide spin labels so useful in biochemistry. The ESR spectrum of a nitroxide spin label depends in a complex manner on both the rate and the symmetry of rotation of the nitroxide group.

The rate of tumbling for a molecule undergoing Brownian motion can be expressed in terms of a correlation time  $\tau$  (Griffith and Waggoner 1969). A naïve definition of  $\tau$  is simply the average time required for a nitroxide to rotate through a significant arc (say  $40^\circ$ ).  $\tau$  is inversely related to the tumbling rate of the molecule and it should be in the range between  $10^{-7}$  and  $10^{-11}$  sec. At rotation greater than  $10^{-11}$  sec, the asymmetrical features in the spectra are averaged out completely, resulting in a narrow three line spectrum. At rotation rates slower than  $10^{-7}$  sec, the spectrum closely resembles that of a completely immobilized free radical. The aim of many calculations is to relate the ESR line shapes to the parameter  $\tau$ .

The most useful approaches to study anisotropic motions are available for the particular situation where the spin label is associated with a molecular system in which there is a rotation about one long axis and one short axis (axial symmetry) (Swartz and Swartz). This motion is typical of, for example, a spin-labelled lipid in a membrane. Thus, asymmetrical rotation such as one might expect in a long, narrow molecule produces characteristic changes in the ESR spectrum that indicate that this molecule is rotating about its long axis in preference to tumbling about one of its short axes. ESR spectra change from the situation where the only possible motion is rotation along the long axis of the fatty acid spin label (order parameter  $S=1$ ) to the entirely random orientation ( $S=0$ ). For example, if the viscosity of the solution is increased, the rotational motion of the nitroxides decreases and the spectra become increasingly asymmetric.

To study our protein system, we used spin-labelled fatty acids and, in particular, 7-DOXYL stearic acid (DOXYL=4,4-dimethyloxazolidine-N-oxy) and 4-PROXYL palmitic acid (PROXYL=2,2,5,5-tetramethylpyrrolidin-N-oxy). The first one is commercially available from the company TCI Europe Ltd, Belgium, the second was a kind gift from Prof. Hideg, Hungary.

a)



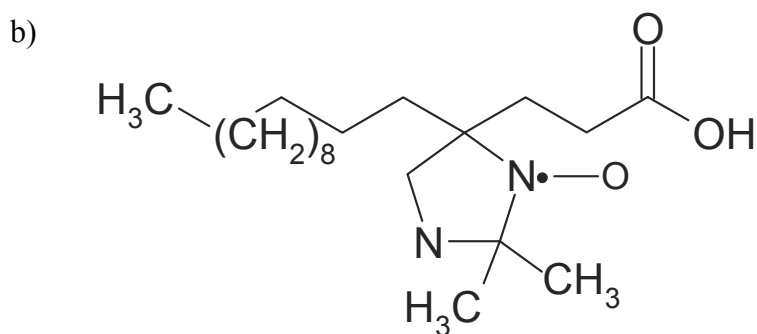


**Fig.1.10:** a) Structure of 7-DOXYL stearic acid; b) Structure of 4-PROXYL palmitic acid.

### The instrument

ESR spectra were measured on a Bruker Elexsys E580 spectrometer, operating in the X-band mode (9.7 GHz). Essential components of a simple ESR spectrometer are a microwave source (a klystron or, nowadays, a Gunn diode), a magnet and a detector (Fig.1.11). The electromagnetic source and the detector are in a box called “microwave bridge”; the sample is held in a quartz capillary tube, with an internal diameter of 1mm or 0.6mm, and placed in a microwave cavity, which is a metal box that helps to amplify weak signals from the sample (Berliner 1976, 1979).

The Bruker EPR spectrometer used is a reflection spectrometer: it measures the changes - due to spectroscopic transitions - in the amount of radiation reflected back from the microwave cavity containing the sample. The detector has to see only the microwave radiation coming back from the cavity. A Schottky barrier diode is used to detect the reflected microwaves: it converts the microwave power to an electrical current.

During the experiment the frequency of radiation is fixed and the magnetic field is scanned. The required magnetic field for the study of free radicals at ~9 GHz is about 3200 Gauss and it is readily achieved with conventional electromagnets. As the resonance condition is approached the sample absorbs microwave energy and we see the peak in the spectrum.

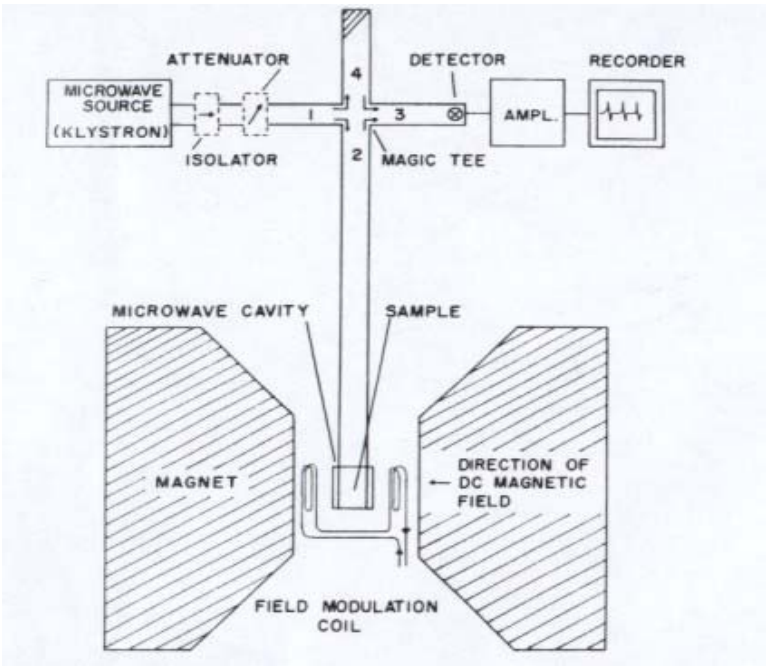


Fig. 1.11: Block diagram of a simple ESR spectrometer.

## OBJECTIVE

The uncoupling proteins (UCPs) are transporters, present in the mitochondrial inner membrane, that mediate a regulated discharge of the proton gradient that is generated by the respiratory chain. This energy-dissipatory mechanism can serve functions such as thermogenesis, maintenance of the redox balance, or reduction in the production of reactive oxygen species. Some UCP homologs may not act as true uncouplers, however, and their activity has yet to be defined. Uncoupling proteins are a unique group of closely related proteins that may play important roles in obesity, diabetes, fatty acid metabolism, and neurodegeneration. The UCPs are integral membrane proteins, each with a molecular mass of 31-34 kDa and a tripartite structure in which a region of around 100 residues is repeated three times; each repeat codes for two transmembrane segments and a long hydrophilic loop. The functional carrier unit is a homodimer. So far, 45 genes encoding members of the UCP family have been described, and they can be grouped into six families. Most of the described genes are from mammals, but UCP genes have also been found in fish, birds and plants, and there is also functional evidence to suggest their presence in fungi and protozoa. UCPs are encoded in their mature form by nuclear genes and, unlike many nuclear-encoded mitochondrial proteins, they lack a cleavable mitochondrial import signal. The information for mitochondrial targeting resides in the first loop that protrudes into the mitochondrial matrix; the second matrix loop is essential for insertion of the protein into the inner mitochondrial membrane. The UCP proteins are composed of six membrane spanning alpha helices, and both the C and N terminus protrude from the cytosolic side of the mitochondrial inner membrane. This is only a secondary structure prediction as the structure of the protein is not yet known. UCPs are regulated at both the transcriptional level and by activation and inhibition in the mitochondrion.

Uncoupling protein 1 was discovered from functional studies of brown adipose tissue mitochondria and was one of the earliest membrane proteins to be sequenced. Several important observations lead to the discovery of UCP1. This protein was originally named “thermogenin” but now is more commonly known as uncoupling protein 1. UCP1 was originally thought to be a unique protein found only in mammalian brown adipose tissue, but further research has revealed at least five uncoupling proteins. UCP1 is considered the classic uncoupling protein, and considerable research has linked UCP1 with cold induced

thermogenesis and is found exclusively in brown adipose tissue. Mammals have five UCP homologs, of which UCP1-UCP3 are closely related, while UCP4 also known as brain mitochondrial carrier protein (BMCP1) expressed only in the brain, physiological function largely unknown, is more divergent. UCP2 was discovered in 1997 and shares 58% sequence homology with UCP1 and 80% with UCP3.

Unlike UCP1, UCP2 is expressed ubiquitously in mammalian tissues and is believed to be a peripheral target for energy dissipation and may have roles in body weight regulation. However, there has been considerable debate about the functions associated with UCP2. Recent evidence from Jaburek *et al.* seems to support their role as uncouplers because ion fluxes of purified UCP2 and UCP3 were identical to UCP1 suggesting that these are functioning uncoupling proteins with a physiological role in energy dissipation. However, establishing physiological roles for UCP2 and UCP3 may be dependent upon improved experimental technique, as current methods have proven insufficient to answer questions regarding the structure and functional relationship of these novel proteins. Many studies of UCP1 relied on expression of the protein in yeast, however, because UCP2 and UCP3 only occur in low concentrations they must be over-expressed in yeast or *E. coli*. Although this technique proved highly successful with UCP1 it does not appear to work with UCP2 or UCP3 because they are not in native conformations when expressed in *E. coli* or yeast.

The function mediated by classic uncoupling protein1 in energy dissipation was explained by Ježek *et al.* Considering the studies of Jaburek *et al.* as elementary, we started to study the function of UCP2. During this course we have studied the foray of reactions catalysed by UCP2 and at the same time also deduced a reliable experimental technique for the over-expression of UCP2 and to isolate it in native conformations. Virtually nothing is known about the transport functions of UCP2 and UCP3, and their putative physiological functions have been deduced primarily from their striking sequence homology with UCP1. Addressing this problem was one of the major tasks, which is discussed in this present work. The protein was expressed in *E.coli* and aggregated into inclusion bodies, by which method we achieved sufficient amounts of protein for our experiments. The main objective of our work was to explain how the energy dissipation and heat generation is catalyzed by back-flux of protons into the mitochondrial matrix, probably by fatty acid cycling mechanism. We have reconstituted the protein into detergent liposomes and measured the fatty acid cycling mechanism with a myriad of substrates and competitors. In addition to this we also planned to

deduce whether fatty acid dependent proton transport by UCP2 was inhibited by purine nucleotides, albeit with lower apparent affinities than observed with UCP1 by Ježek *et al*, in order to evaluate that UCP2 is a functional uncoupling protein and that its biophysical properties are consistent with a physiological role in energy dissipation.

**ABBREVIATIONS**

AA	Arachidonic acid
ADP	Adenosinediphosphate
ATP	Adenosinetriphosphate
BAT	Brown adipose tissue
BMCP	Brown mitochondrial carrier protein
BSA	Bovine serum albumin
C <sub>12</sub> E <sub>9</sub>	Nonaethylene glycol monododecyl ether
db	decibel
DSA	DOXYL stearic acid
DTT	Dithiothreitol
DOXYL	4,4-dimethyloxazolidine-N-oxyl
EST	Expressed sequence tags
EDTA	Ethylenedinitrilotetraaceticacid
EPR/ESR	Electron paramagnetic/spin resonance
ETA	Eicosatrienoic acid
FA	Fatty acid
G	Gauss
GDP	Guaninediphosphate
GHz	Giga hertz
HLA	12-hydroxy lauric acid
HNE	4-hydroxy nonenal
IB	Inclusion bodies
IPTG	Isopropyl- $\beta$ ,D-thiogalactopyranoside
K	Kelvin
kDa	kilo dalton
NO group	nitric oxide group
OA	Oleic acid
ODS	Octadecane sulfonate
PA	Palmitic acid
PA buffer	Phospho Acetate buffer

PMSF	Phenylmethylsulfonylflouride
PN	Purine nucleotides
PPA	PROXYL palmitic acid
PROXYL	2,2,5,5-tetramethylpyrrolidin-N-oxyl
ROS	Reactive oxygen species
SDS	Sodium dodecyl sulphate
SL	Spin label
SLFA	Spin-labelled fatty acid
SLS	Sodium N-lauroylsarcosine
TCA	Tri chloroacetic acid
TE buffer	TRIS-EDTA buffer
TRIS	Tris (hydroxymethyl) aminomethane
UCP	Uncoupling protein
UDS	Undecane sulfonate

## METHODS

### Expression of uncoupling protein in E.coli –

Human uncoupling protein 2 (UCP2) open reading frames were amplified by PCR and inserted into the *NdeI* and *NotI* sites of the pET21a vector (Novagen). By DNA sequencing, the construct is predicted to encode protein with an amino acid sequence identical to the wild type UCP2 protein. Plasmids were transformed into bacterial strain BL21 (Novagen). The cloning of UCP2 plasmid was done by Martin Jaburek (protocol published), the protein expression and below mentioned inclusion bodies isolation was performed in Prague at the department of Dr.Ježek. The transformed cells were used for bacterial expression of uncoupling protein and its isolation in inclusion bodies.

### Solutions and Media:

2 x YT medium:	Bacto-tryptone	8gm
	Bacto-yeast extract	5gm
	sodium chloride	2.5gm
	distilled H <sub>2</sub> O	500ml (dissolve first in 450ml)

Shake until the solutes have dissolved and adjust the pH to 7.0 with 1N sodium hydroxide (NaOH). Make up the final volume to 500ml with distilled H<sub>2</sub>O. Sterilize the medium by autoclaving for 20 minutes at 120mb atm pr.

PA buffer:	phosphate (Na <sup>+</sup> salts)	150mM
	EDTA	25mM
	ethylene glycol	5% (w/v)
	pH – 7.9	

add 1mM DTT and 2mM PMSF just prior to use.

Carbenicillin: Na salt, use 100µg/ml final concentration

IPTG: 0.5M stock solution.

Dissolve 1.2gm of IPTG (isopropyl- $\beta$ -D-thiogalactopyranoside) in 10 ml of distilled H<sub>2</sub>O and filter sterilize the solution by passing through a 0.22 micron disposable filter. 1ml aliquots are stored at -20°C.

TE buffer:                    TRIS                    100mM  
                                  EDTA                    1mM  
                                  pH – 7.8 (adjust by 1N HCl)  
                                  add 1mM DTT and 2mM PMSF just prior to use.

Procedure:

- 1) Prepare 0.5 lit of 2 x YT medium, and add carbenicillin at a final concentration of 100 $\mu$ g/ml.
- 2) Always start from the frozen stock –  
Scrape a few microliters from the surface with inoculation loop, return the culture to -80°C freezer without thawing.  
Plate this E.coli on 2 x YT plates containing carbenicillin. Incubate overnight at 37°C.
- 3) Grow small culture from single bacterial colony in 3ml of 2 X YT medium containing carbenicillin. Incubate at 20°C over night.
- 4) Inoculate the 0.5 lit of 2 x YT medium with 2ml of overnight culture from above step, incubate the medium at 37°C with aeration, until A<sub>600</sub> reaches 0.3 – 0.4.
- 5) Induce the expression in the medium by adding IPTG to a final concentration of 1mM. Continue incubation at 30°C with aeration for 3 – 4 hours.

All following steps are carried out at 4°C –

- 6) Harvest the cells using a GSA rotor. Centrifuge 2 x 250 ml of the cell culture at 500 x g for 15 min. (store at -20°C.)
- 7) Suspend the cell pellet in 20 ml of ice-cold TE buffer and pass it twice through a pre-cooled French pressure cell. The resulting lysate is centrifuged 2 x 10 ml at 27,000 x g for 15 min ( or 20,000 x g for 25 min), using a SS34 rotor.
- 8) The pellet is homogenized in TE medium, centrifuge at 1,000 x g for 3 min. Regain the supernatant from this step.

- 9) Centrifuge the supernatant from above step at 14,000 x g for 15 min.
- 10) Weigh the resulting final pellet (inclusion bodies):
- 11) Resuspend the pellet with PA buffer and centrifuge 1 ml aliquots of the resulting suspension at 14,000 x g for 15 min in a microcentrifuge.

Volume of PA buffer used for resuspension:

- 12) Store the pelleted inclusion bodies from above centrifuge step frozen at -70°C.

[Note: The inclusion bodies become less soluble upon aging in freezer.]

#### Solubilization and refolding of uncoupling protein from inclusion bodies –

To refold bacterially expressed uncoupling protein by functional reconstitution to its native conformation for binding studies.

#### Solutions and chemicals:

PA buffer:                   phosphate (Na<sup>+</sup> salts) 150mM  
                                  EDTA                        25mM  
                                  ethylene glycol        5% (w/v)  
                                  pH – 7.9  
                                  add 10mM DTT and 2mM PMSF just prior to use.

TE buffer:                   TRIS                        100mM  
                                  EDTA                        1mM  
                                  glycerol                 10% (w/v)  
                                  pH – 7.8 (adjust by 1N HCl)

Solubilization buffer: 2% (w/v) SLS dissolved in TE buffer.  
                                  Add 1mM DTT and 0.2mM PMSF just prior to use.

Dialysis buffer:            Internal medium for a given experiment.

## Procedure:

All steps are performed at 4°C unless stated otherwise –

- 1) Wash inclusion bodies to remove loosely bound protein contaminants: resuspend each inclusion bodies eppendorf in 1 ml of PA buffer and 2% Triton X 100.  
Centrifuge at 14,000 x g for 10 min in a microcentrifuge. Discard supernatant carefully.
- 2) Repeat the wash step. Add 1 ml PA buffer and 0.2% solubilization buffer to the pellet. Resuspend it and centrifuge at 14,000 x g for 10 min.
- 3) Solubilize inclusion bodies: Add 1 ml of solubilization buffer to the resulting pellet from above step. Vortex well and use gentle pipetting to resuspend inclusion bodies to homogeneity.  
The above resuspended solution is incubated at room temperature for 15 min with occasional vortexing and gentle pipetting.
- 4) Dilute this solution with TE buffer 4 fold (final volume 4 ml) and vortex. Centrifuge the suspension at 14,000 x g for 10 min to remove unsolubilized particles.
- 5) Allow the supernatant to stand at 4°C, and simultaneously prepare refolding buffer.
- 6) Prepare 6 ml of TE buffer with 0.1% C<sub>12</sub>E<sub>9</sub> containing 1mM DTT and 0.1mM ATP final concentration, vortexed and mixed to homogeneity. (This is refolding buffer.)
- 7) Dilute the supernatant from step 5 with the refolding buffer sequentially by adding 500µl aliquots, every 30 min interval between each additions.

[Final volume of resulting solution 10 ml]

- 8) Dialyze the sample against TE buffer containing 0.1mM DTT, 0.1mM ATP, 1 gm BSA and 0.1% C<sub>12</sub>E<sub>9</sub> for overnight at 1:100 dilution (1 lit).
- 9) Now dialyze the sample with a fresh dialysis buffer for 8 – 9 hours.
- 10) Final dialysis is performed against only TE buffer containing 0.1 % C<sub>12</sub>E<sub>9</sub> for overnight.
- 11) Concentrate the sample to ~1 – 2 ml, using the ultrafree–15 centrifugal filter device (Millipore).
- 12) Centrifuge the resulting concentrate at 14,000 x g for 10 min to remove any precipitate.

13) Store the protein at  $-20^{\circ}\text{C}$  or proceed to following step.

14) The amount of protein is estimated by Lowry's and BCA methods.

Measure the volume of sample:

15) The estimated protein is then concentrated to desired quantities using centricon or vivaspin-6 centrifugal devices.

Reconstitution of bacterially expressed uncoupling protein into proteoliposomes.

The functional reconstitution and solubilization of uncoupling protein is carried out by the same method as described above along with few additional solutions and steps as described below.

Solutions and chemicals:

Phospholipids: E.coli phospholipids (100mg/ml in chloroform) dried under nitrogen, stored under vacuum. (use  $\sim 10\text{mg/mg}$  protein)

All other buffers required are same as described in previous method.

Procedure:

The following steps are carried on after the concentration of protein followed by dialysis as discussed above.

[Note: Phospholipids ( $\sim 10\text{mg/mg}$  protein) are added in the refolding buffer, vortexed and sonicated to homogeneity.]

## Hydroxyapatite treatment –

- 1) For each ~2mg of protein aliquot, prepare 0.4mg of hydroxyapatite (HTP) in a column.
- 2) Wash the column by letting at least 10ml of the dialysis buffer pass through and spin 500 x g for 1 min to remove residual medium.
- 3) Now load the sealed HTP column with the protein solution and let sample pass through gravity.
- 4) Spin the column at 500 x g for 1 min to collect the remaining sample.

## Bio beads treatment –

Prepare 2 x 2.5 ml of pre-washed bio beads (in distilled water or ethanol) columns:

- a. Seal two 5cc syringes with fibreglass.
  - b. Remove water or ethanol from bio beads by centrifugation at 800 x g for 1-2 mins.
  - c. Wash the bio beads in syringes with dialysis buffer using a volume 4 to 5 times the packed volume.
  - d. Seal the syringe outlet, apply more dialysis buffer and let equilibrate over night.
- 1) Remove 0.5 ml of the pre-equilibrated bio beads to a separate syringe sealed with fibre glass.
  - 2) Spin the syringe at 800 x g for 2 min to remove residual medium and seal the outlet.
  - 3) Add the protein sample to the syringe and incubate the mixture at 4°C for 30 min.
  - 4) At every consecutive 30 min interval keep adding the bio beads to the syringe by preparing as in step 1.
  - 5) Repeat the steps until the final volume of bio beads is 2 ml.
  - 6) Separate the proteoliposomes from bio beads by centrifuging at 800 x g for 2 mins.
  - 7) Add the proteoliposomes to a fresh prepared bio beads column as described in step 1 and incubate for additional 30 – 60 mins.
  - 8) Now centrifuge column at 800 x g for 2 mins.
  - 9) Measure the volume of resultant proteoliposomes.

V =

10) Estimate the protein concentration in the proteoliposomes.

P =

Amido Black protein estimation –

The procedure is used to determine microgram quantities of protein in the presence of milligram levels of lipids.

Solutions and chemicals:

10% (w/v) SDS

100% (w/v) TCA

6% (w/v) TCA

1 M TRIS in 1% (w/v) SDS medium, pH 7.5

Staining solution: 0.1% (w/v) Amido Black 10B dissolved in methanol/acetic acid/  
distilled water (v/v/v 90/2/8)

Destaining solution: methanol/acetic acid/ water (v/v/v 90/2/8)

25mM NaOH/0.05mM EDTA/ 50% (v/v) ethanol.

Calibrated 0.2 mg/ml BSA.

Materials:

Millipore filters (0.45µm pore size)

Millipore filtration system connected with vacuum

Procedure:

Preparation of Millipore filters –

- 1) Number each filter at the edge, taking care of the surface of the filter.
- 2) Soak the filters in distilled water until use.

- 3) Place filters with labelled side facing bottom on the filtration system.
- 4) Place flange over filters, careful not to rip filters.
- 5) Remove water just prior to use.

Prepare standards and samples for estimation –

- 1) Dilute the protein samples and standards to final volume of 2 ml with distilled water in separate tubes.
- 2) Add each sequentially to the samples, letting follow thorough vortexing of mixture-
  - a. 0.2 ml 10% SDS
  - b. 0.3 ml 1 M TRIS in 1% (w/v) SDS medium, pH 7.5
  - c. 0.6 ml 100% (w/v) TCA
- 3) Incubate the samples for 3 – 4 mins.
- 4) Transfer the samples to above numbered filters and dry filter under vacuum.
- 5) Wash filters with 2 ml of 6% (w/v) TCA, vacuum-dry thoroughly.
- 6) Remove filters and soak in 200 ml of staining solution for 3 mins.
- 7) Rinse filters quickly with 200 ml distilled water
- 8) Wash filters in 200 ml destaining solution for 3 times with 1 min each wash.
- 9) Again rinse filters in 200 ml distilled water for 2 mins.
- 10) Place filters on wipes with stained side up and soak residual water.
- 11) Add 0.7 ml of 25mM NaOH/0.05mM EDTA/ 50% (v/v) ethanol to each filter and incubate for 20 mins with occasional vortexing.
- 12) Collect solution in microcuvettes and measure absorbancies at 630 nm wavelength.

Tablesheets for an amido black protein assay:

Sample	Sample Amount	Sample Conc ( $\mu\text{g}$ )	Distilled water	10% SDS	1M TRIS/ 1% SDS	100%TCA
Standard	--	--	2000	200	300	600
Standard	10	2	1990			
Standard	50	10	1950			
Standard	100	20	1900			
Sample	25	?	1975			
Sample	50	?	1950			

Number of samples can be duplicated for better estimates.

[Note: Volume in microlitres ( $\mu\text{l}$ )]

#### Protein determination –

Total protein determination was used for the inclusion bodies preparation as well as also for the reconstituted protein. While BCA test (BIORAD kit) was used for the amount of protein in inclusion bodies, the total protein after reconstitution was estimated using Lowry's method.

Using the BCA method the amount of protein in each aliquot of inclusion bodies freezed was standardized to ~2mg per eppendorf.

#### EPR measurements –

EPR spectra were measured on a Bruker Eleksys E580 EPR spectrometer, operating in X-band mode (9.7 GHz). A dielectric cavity was used as the microwave source for experiments. Typically, 60 $\mu\text{l}$  or 30 $\mu\text{l}$  aliquots of solubilized UCP2 in C<sub>12</sub>E<sub>9</sub> micelles were incubated with 4-fold excess of spin-labelled fatty acid. EPR spectra of the samples at 293K were obtained by averaging of atleast 2 to 3 scans with a scan width of 100 gauss at a centre field of 3452 G. The microwave power was set to 8mW, receiver gain of 64db to 72db with modulation amplitude of 1G. Intensities were adjusted by auto baseline correction.

The parameters described above were established after a set of reasonable tuning conditions for the clear representation of bound regions in the spectra, the small scan width region spectrums of the bound regions only shown in some figures as overlay were recorded with better signal to noise ratio settings for better visibility.

**MATERIALS**

Avanti Polarlipids:	Lecithin (soya bean)
Becton Dickinson (BD):	Bacto tryptone Bacto yeast extract
Biorad:	Amido Black 10B BCA kit Bio beads SM2 absorbent
Gerbu:	Carbenicillin Dithiothreitol IPTG
J T Baker:	Hydrochloric acid
Millipore:	0.22 micron filters Filtration system with vacuum
Merck:	NaOH NaH <sub>2</sub> PO <sub>4</sub> EDTA Ethylene glycol Glycerol Folin ciocalteus phenol reagent
Omni fix:	1 ml syringes 0.45 micron filters
Roche:	ATP SDS
ROTH:	Sodium chloride
Sarstedt:	0.22 micron filters (for sterilization)
Sigma:	BSA (Fraction V) CTC TRIS PMSF SLS C12E9 Triton X-100

Phospholipids

HTP

Dowex 11A8 Retardion

TCA

Serva:

DOC

Ethanol, methanol and acetic acid are of analytical grade from department chemicals facility.

Microfuge centrifuge – Eppendorf

Centrifuge – Beckman J2-21 model, Rotors used JA20.

Spectrophotometer – Beckman DU640.

Frenchpress – Sim Aminco SLM Instruments Inc.

Vector – pET21a (Novagen)

Competent cells – BL21 DE3 (Novagen)

## RESULTS and DISCUSSIONS

EPR spectroscopy is a significant biophysical technique that specifically detects unpaired electrons. Because the natural occurrence of such paramagnetic species in biological systems is relatively low, ESR sensitive reporter groups (spin labels or spin probes) can be introduced chemically into biological systems, either through chemical modification of the bio-molecule or via spin-labelled substrates or cofactors. The method is highly sensitive to conformational transitions within the vicinity of these reporter groups and therefore allows the evaluation of conformational/structural processes during substrate binding and often during enzymatic turnover. ESR is of great significance for studies of membrane proteins where many other biophysical methods are “relatively handicapped” due to the specific characteristics of membrane biology, e.g., ESR is unaffected by light scattering, and it can also be used at high viscosities of the samples. Furthermore, the relatively small size of the spin label usually does not significantly perturb the biological activity of the enzyme or protein. Requirements, however, are large amounts of protein and rather high protein concentrations (usually  $> 15\mu\text{M}$ ) that are needed for acceptable signal/noise ratio of the resulting ESR spectra. Especially for membrane proteins this could be difficult to obtain, but for NMR studies it is even a tough task filling step where the concentrations requirement is 1000 fold more due to the magnetic moments of electrons being higher than that of protons.

The development of the solubilization/reconstitution from inclusion bodies allowed us to achieve adequate yields and functionally refolded protein for ESR spectroscopy, therefore allowing the use of this powerful biophysical technique to study this enzyme. In the present study hUCP2 has been isolated from inclusion bodies by solubilizing it in the non ionic detergent nonaethylene glycol monododecyl ether ( $\text{C}_{12}\text{E}_9$ ), as mentioned in detail in previous chapters, to support our hypothesis which has been postulated by Garlid and Ježek long back that uncoupling protein (UCP) probably mediates fatty acid cycling across the membrane by transporting anionic fatty acids which then flip-flop back via the lipid bilayer in a protonated form. In order to show that the substrate for UCP is fatty acids, we successfully used spin-labelled fatty acids (SLFA) to study binding in soluble proteins. DOXYL stearic acid and PROXYL palmitic acid (kind gift from Prof.Hideg) were found to be our most useful probes for demonstrating the fatty acid cycling across the membrane. However we have to accept the truth that our method of solubilization or isolation of protein results in only 80% of active refolded protein and only partially mimics the *in-vivo* environment. The binding of spin-

labelled fatty acid to the concentrated UCP clearly reveals the significance in our protein isolation method and on the other hand allowed us to study the competition with other substrates and ligands of UCP. In this study, we used spin-labelled fatty acids, contains a stable nitroxide radical attached at different positions along the chain of fatty acid. These spin probes have been successfully used in previous studies and demonstrated the binding with UCP [Ježek *et al* 1995]. We have been able to record EPR spectra of 4-PROXYL-palmitic acid (4-PPA) and 5-DOXYL-stearic acid (5-DOSA) bound to UCP which clearly showed separated peaks representing the bound and partially free spin-label components in the respective “low-field” and “high-field” regions of EPR spectra, whilst with 7-DOXYL-stearic acid (7-DOSA) the separated peaks were smoothed into one wide peak.

### **Spin-labelled fatty acid, an excellent substrate-**

Spin-labelled fatty acid (SLFA) is an excellent substrate to study binding and fatty acid cycling via the lipid bilayer in a protonated form, with competing substrates and ligands of UCP. The use of spin-labelled fatty acids gives some insight about the protein, one being the affirmative proof of binding site for the fatty acid in the protein, and another the competitive effects of different kinds of fatty acids. As we know that fatty acids are classified into active saturated and unsaturated fatty acids and inactive fatty acids. Competition studies with some of these fatty acids on UCP bound to SLFA reveal some information on the regulation and mechanism of the protein. Standardization of the protein/lipid ratio was one of the most important aspects in our studies in order to achieve a demonstrable bound component in the spectrum.

The spectrum of a certain spin-labelled fatty acid bound with protein clearly differs from that only in micelles without protein which can be shown by accurate determination of the  $2A_{zz}$  parameter. This was on average  $45.2 \pm 0.6$  gauss ( $n=8$ ) with protein, whereas 4-PPA in 0.1% nonaethylene glycol monododecyl ether ( $C_{12}E_9$ ) exhibited a  $2A_{zz}$  of 34.4 gauss. Figure 3.1 illustrates the EPR spectrum of  $112\mu\text{M}$  4-proxyl palmitic acid bound to  $28\mu\text{M}$  UCP2 in micelles of  $C_{12}E_9$ . The spectrum exhibits clearly separated peaks in the low-field and high-field regions respectively, the two peaks labelled in each region indicate the existence of more or less immobilized spin-labelled fatty acid. Correspondence to the  $h_{+i}$  peak of the immobilized spin probe, distinct from the residual  $h_{+m}$  peak of more freely tumbling species suggests that the former could reflect the population bound to the protein and the later in

micelles. The bound regions of the spectrum were re-recorded at higher signal gain and aligned over the spectrum for better visualization. When the same UCP sample was precipitated with trichloroacetic acid, the bound signal disappeared. The later figure 3.2 depicts the spectrum of 5 and 7 doxyl spin-labelled fatty acids bound to protein. The protein concentration in our preparation varied on an average range of  $25\mu\text{M}$  to  $35\mu\text{M}$ , depending on the yield in our experiments.

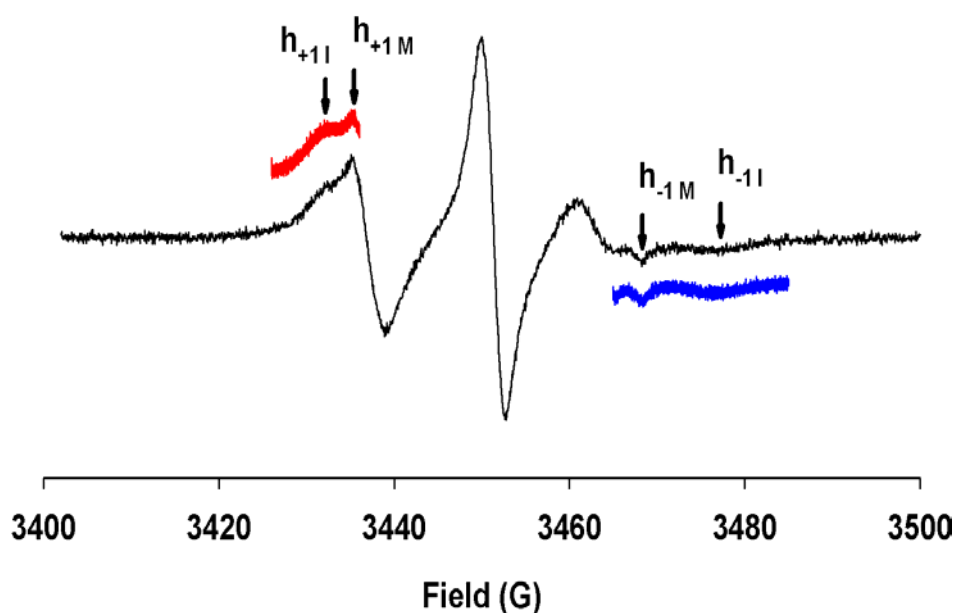


**Fig 3.1:** EPR Spectra of  $112\mu\text{M}$  4-proxyl palmitic acid bound to  $28\mu\text{M}$  UCP2.

The present work gives evidence for the interaction of several spin-labelled fatty acids with mitochondrial uncoupling protein. Even if the viscous micellar environment provides quite an extensive immobilization to spin-labels in the absence of protein, this lower extent immobilization was reflected by peak separation of  $\sim 30$  gauss with a suppressed high-field peak as typical for weakly immobilized nitroxides. UCP2 protein addition caused appearance of additional bound components separated by more than 40 gauss which was observed in all the three kinds of spin-labels, 7 and 5-DOXYL-stearic acid (DSA) and 4-PROXYL-palmitic acid (PPA). Consequently, and after judging of the binding changes, they were evaluated only when we observed variations in these peaks, termed  $h_{+1i}$  and  $h_{-1i}$  according to Marsh *et al.*

Our screening of several spin-labelled fatty acids with different positions of the nitroxyl group with respect to the carboxyl group revealed that it is undoubtedly the carboxyl

group which is bound to UCP2, since no immobilization was observed for the label of 16-DOXYL-stearic acid and  $2A_{zz}$  values for the immobilized spin probes were increasing in the order of 7-DSA < 5-DSA < 4-PPA, thus reflecting higher immobilization for a closer proximity of the nitroxide group to the carboxyl group. In conclusion, we show that spin-labelled fatty acids when bound to UCP2 are highly immobilized close to their carboxyl end. To show the specificity of the UCP2 binding site on which high immobilization of spin probes took place, we have demonstrated competition with few exemplar fatty acids which decreased those peaks in the high field region which correspond to the bound component. This indicates that such competition proceeded on a protein binding site and not within micelles and an additional evidence for physiological function of the protein.

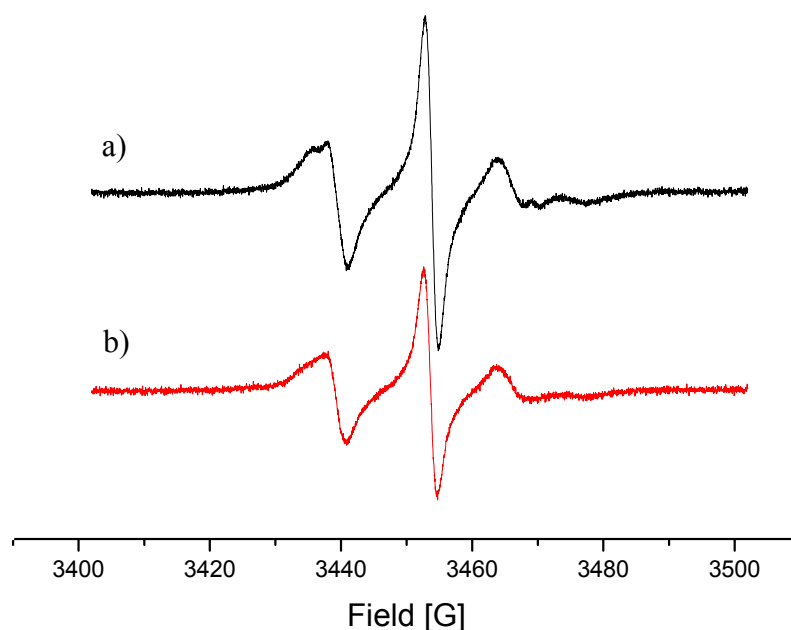


**Fig 3.2:** a) EPR spectra of  $120\mu\text{M}$  5-DOXYL stearic acid bound to  $30\mu\text{M}$  UCP2, b) EPR Spectra of  $120\mu\text{M}$  7-DOXYL stearic acid bound to  $30\mu\text{M}$  UCP2.

One of the main goals of our studies was to explore the functional mechanism of UCP2 which was expected to be the same as of UCP1. This postulation was proved by our studies with different spin-labelled fatty acids. The significance in studying the competition with different fatty acids lies in showing that UCP2 evidently transports monovalent unipolar anions, as does UCP1, and that its role is to dissipate the proton gradient existing between the mitochondrial matrix and the intermembrane space.

It has been known that UCP1 transports monovalent unipolar anions as  $\text{Cl}^-$  (Ježek and Garlid, 1990). In order to answer the question how this protein could transport  $\text{H}^+$  and, in the same time  $\text{Cl}^-$ , an involvement of fatty acids (FAs) in the protonophoric function of UCP1 was proposed (V.P. Skulachev, 1991). It was thought that the resulting net transport of protons was not because the protein simply translocated protons, but because it was able to mediate uniport of anionic fatty acids, while after their passage they became protonated and flipped back with the proton (Ježek *et al.* 1997; Jaburek *et al.* 1999; Jaburek *et al.* 2001; Zackova *et al.* 2003; Ježek *et al.* 2004; Garlid *et al.* 2005). Thus, it was assumed that fatty acids were the proton transporters and that they followed the same pathway as  $\text{Cl}^-$ .

### Competition of natural fatty acids with spin-labelled fatty acid -

The figure below depicts structures of different saturated and unsaturated fatty acids of which some were used for the present study.

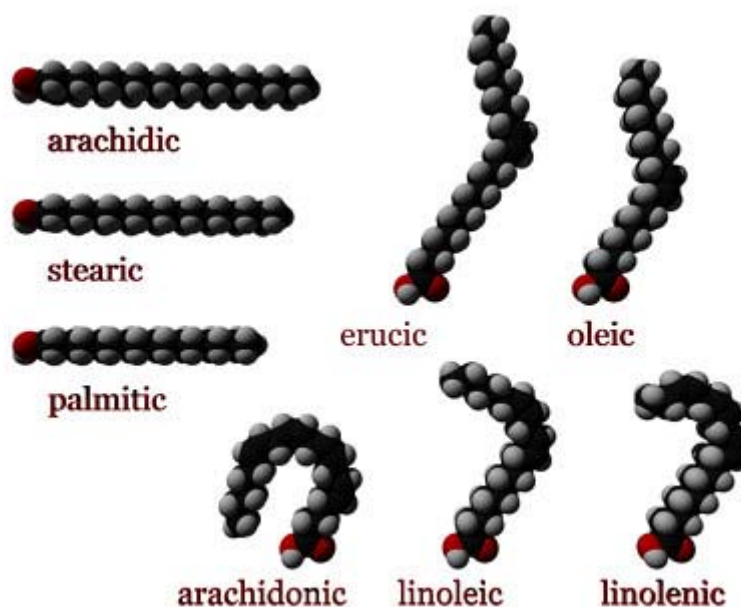


**Fig 3.3:** *Computationally modelled structures of different fatty acids*

We have demonstrated the competition of natural fatty acids which displaced the bound spin-labelled fatty acid from UCP2. The reason behind studying the same exemplar

substrates with all the spin-labelled probes was to give strong affirmative evidence about the presence of a fatty acid binding site on UCP2.

Upon addition of a competing fatty acid to C<sub>12</sub>E<sub>9</sub> micelles, such as dihomogamma linoleic acid i.e. all-cis-8,11,14-eicosatrienoic acid (ETA) or arachidonic acid i.e. all-cis-5,8,11,14-eicosatetraenoic acid (AA) in increasing concentrations, the bound peaks are narrowing and rising in the low-field region, and the double inflection in the high-field region turns into a single one. These changes explain that probably arise from the redistribution of both fatty acids, the spin probe and the added fatty acid, between the micelles and solution in a way that the spin label becomes moving more freely, most probably being released into the aqueous medium.

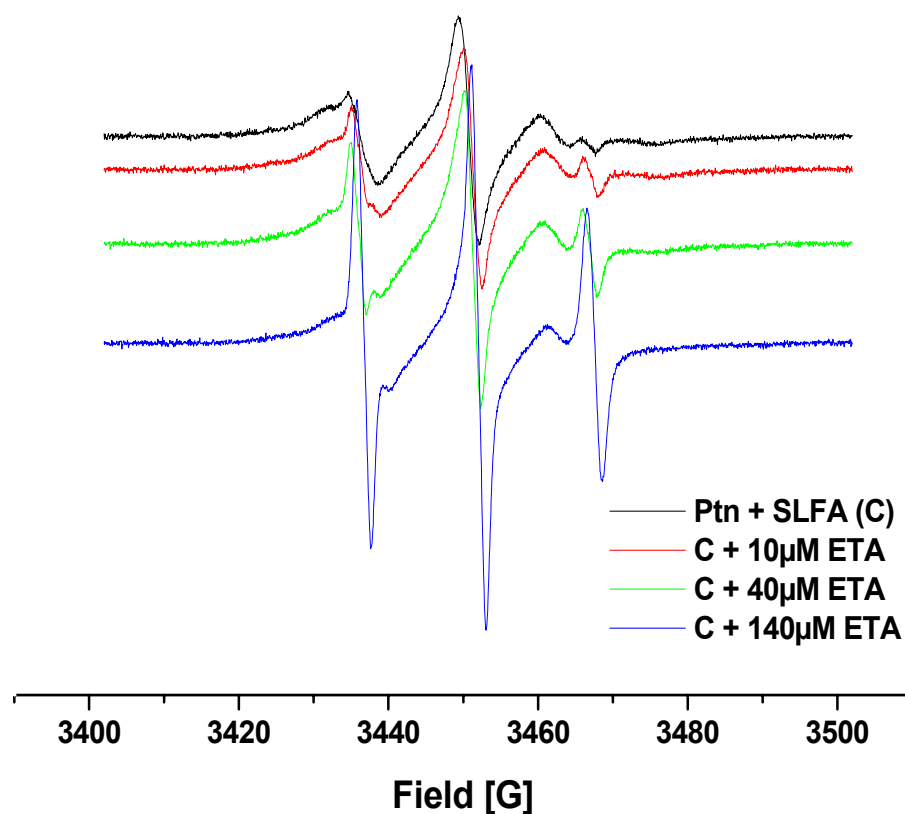


**Fig 3.4:** Illustrates the competition of added eicosatrienoic acid on 5-DSA bound to UCP2.

The competition with palmitic acid (PA) exhibited affinities with slightly higher concentrations than that of the spin probe, however the present concentrations of the added fatty acids still suggests us the significance in the mechanism of UCP2. In previous studies

with UCP1 the reported competition of palmitic acid with 5-DSA on UCP1 showed the displacement at the millimolar range. But, still though physiological significance lies in the difference from millimolar concentrations to that of micromolar concentrations in the present study, it has to be considered that the exact  $K_d$  values can't be estimated. So the  $K_d$  values mentioned in the tables in the present chapter are an approximate estimation and can be referred to as the upper limit of the mean dissociation constant values.

The competition of added fatty acids was more consistent and can be significantly observed in case of studies with 4-PPA bound to UCP2. We have demonstrated that a competition of 4-PPA with the added fatty acid in the protein free micellar system can only redistribute both spin-label and the added fatty acid between detergent micelles and aqueous phase, which enables for higher mobility of the spin-probe. Simultaneously, we have also shown that in the presence of UCP2 when the spin-label is highly immobilized, the added fatty acid causes decrease of the bound peaks due to release from the protein binding site. The probe is released to the micellar and aqueous environment which results in raising the mobility of the spin-probe in both these phases. This is reflected by the corresponding increasing intensity of the  $h_{+1m}$  and  $h_{-1m}$  peaks respectively.

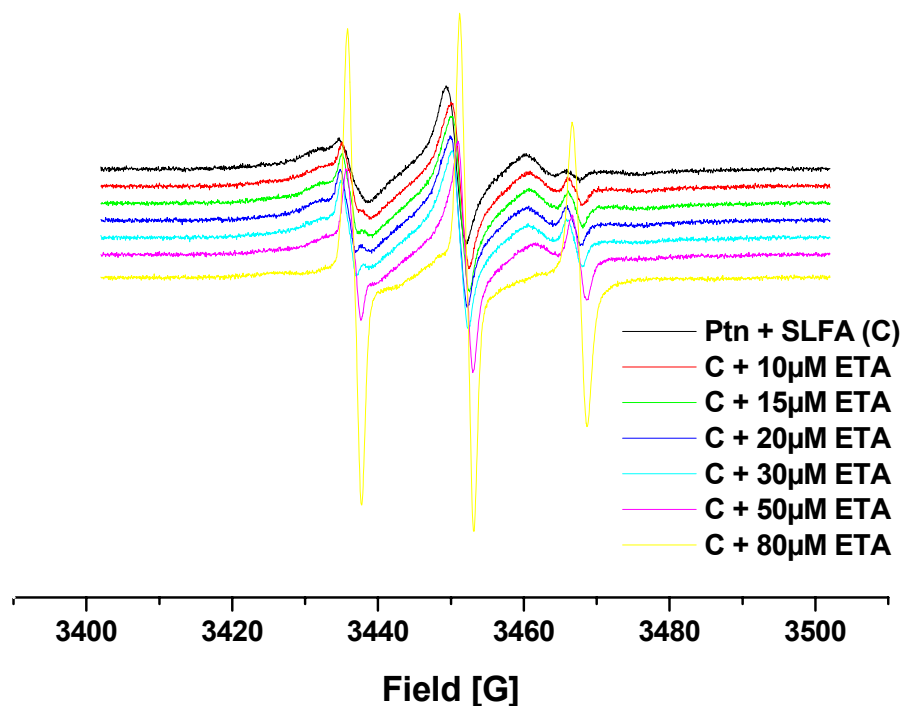


**Fig 3.5:** Illustrates the competition of eicosatrienoic acid over 4-PPA bound to UCP2.

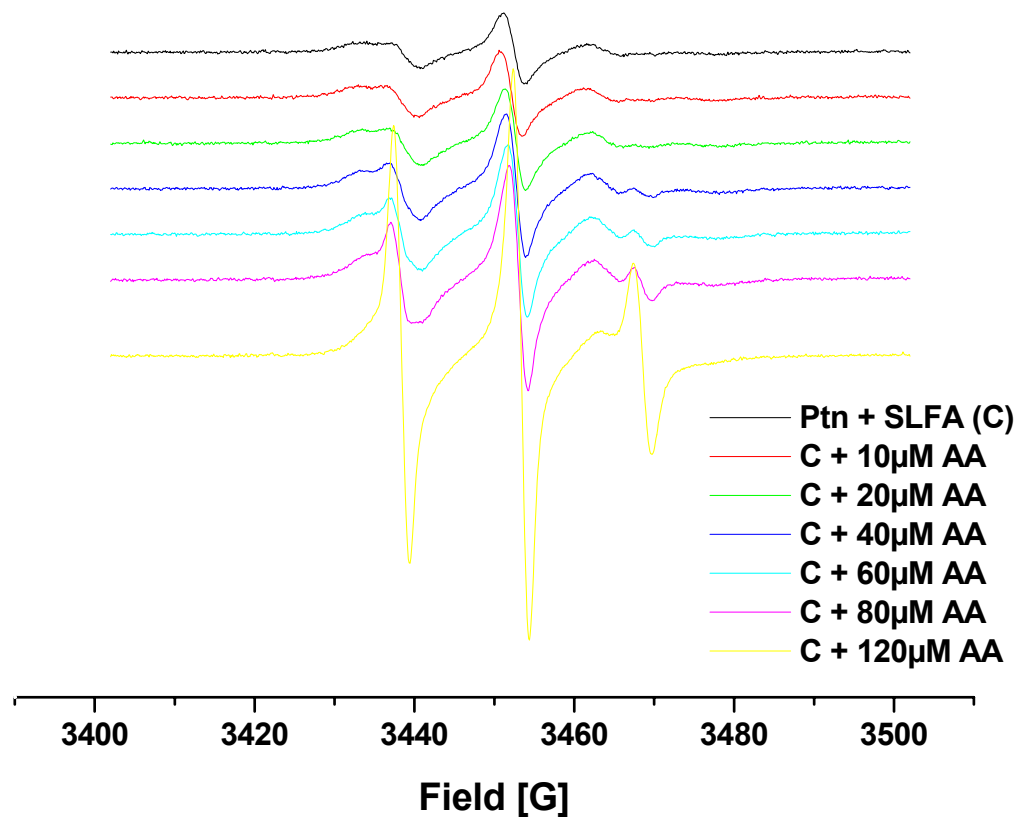


**Fig 3.6:** Illustrates the competition of arachidonic acid with 4-PPA bound to UCP2.

Arachidonic acid and eicosatrienoic acid, with slightly lower affinities than compared with palmitic and oleic acid, exhibited competition in concentrations lower than that of the spin probe, which suggest their high affinities to UCP2. In conclusion, by the competition of palmitic acid, oleic acid, arachidonic acid and eicosatrienoic acid with 5-DSA and 4-PPA bound to UCP2, a putative fatty acid binding site is observed for mitochondrial uncoupling protein 2.

Fattyacid used	Approx kD
Eicosatrienoicacid	60µM
Arachidonicacid	60µM
Oleicacid	50µM

**Table 3.1:** The approximate dissociation constants concentration of different fattyacids.

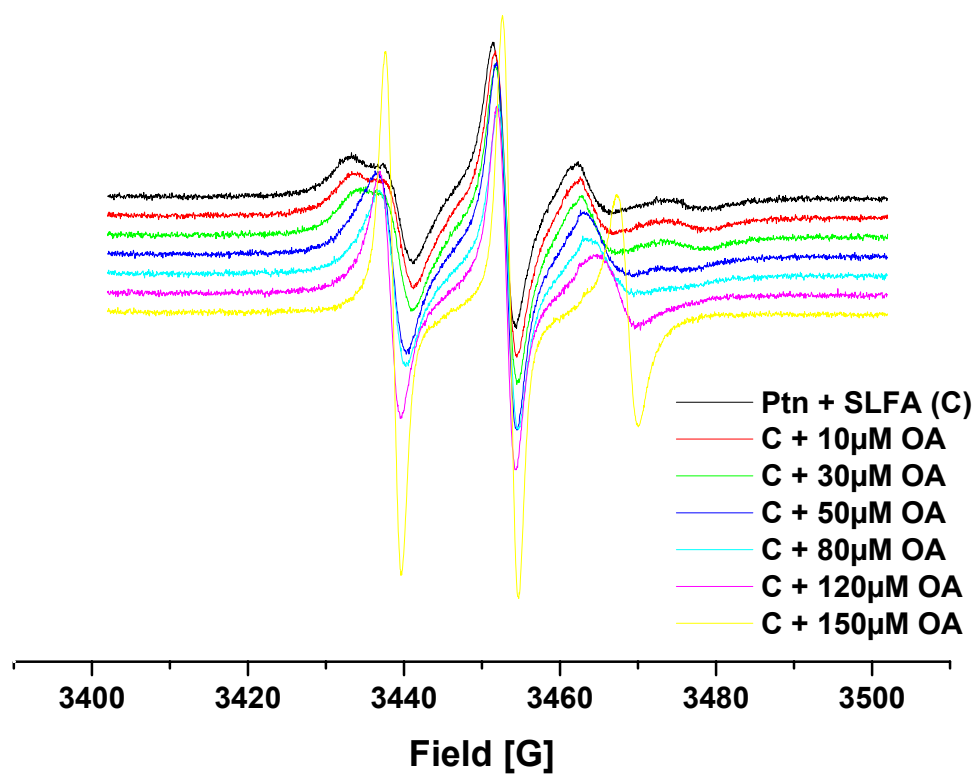
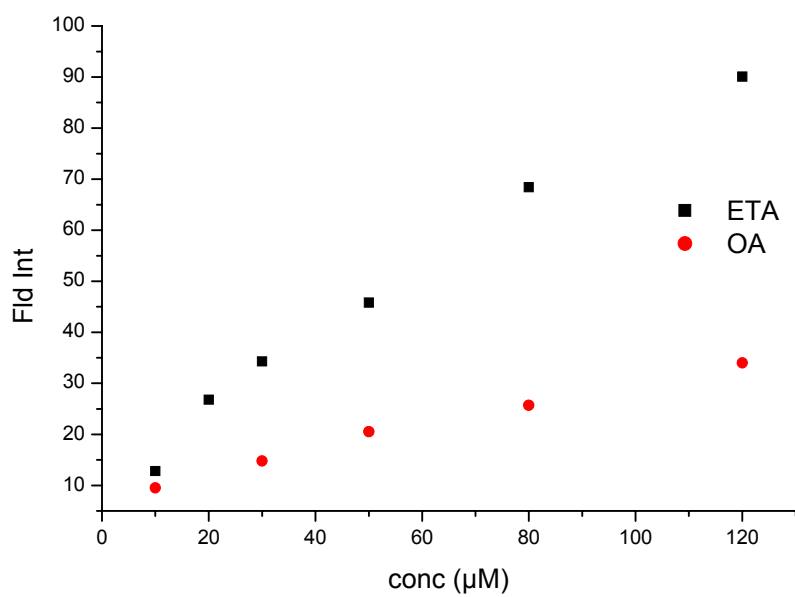
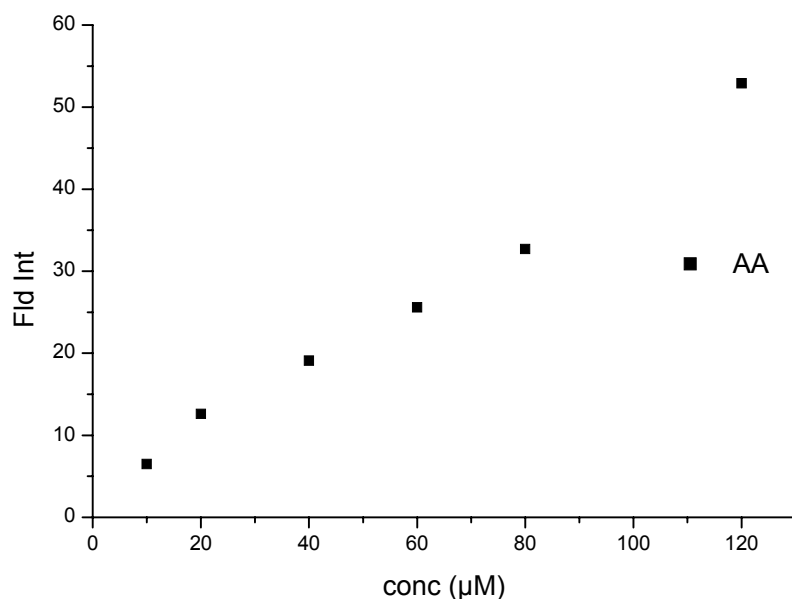


**Fig 3.7:** Illustrates the competition of oleic acid with 4-PPA bound to UCP2.



**Graph 3.1:** Approximate upper limit kD estimation for ETA and OA.



**Graph 3.2:** *Approximate upper limit kD estimation of AA.*

Experiments with brown fat mitochondria in the early 1970s indicated that these mitochondria had an atypical permeability to anions at neutral pH. This anion permeability was soon related to the nucleotide-sensitive uncoupling pathway that was responsible for the thermogenic capacity of the tissue. Ježek and Garlid demonstrated years later that the reconstituted UCP1 could catalyze a GDP-sensitive transport of a wider variety of anions. These observations have ended up in the proposal that fatty acids are also UCP substrates. Therefore, their hypothetical mechanism for the fatty acid activation of thermogenesis would be a protonophoric cycle: the translocation of the anionic form of the fatty acid. Once in the cytosolic side of the membrane, the carboxylate group would pick up a proton and the protonated fatty acid would flip-flop back to the matrix side where the proton would be released and the protonophoric cycle is completed.

### **Alkyl sulfonates as competitors for UCP2 –**

The requirements of the transported substrates do not appear to be very stringent when analyzed with UCP reconstituted in liposomes. They must be monovalent anions, and a

second polar group cannot be present unless it is close to the carboxylate. It has also been described that increasing hydrophobicity also increases the rate of permeation. One intriguing limitation to the transmembrane flip-flop is the presence of bulky-planar structure of the benzene ring at the end of the tail and thus, a compound like phenyl-hexanoic acid does not permeate so easily.

Alkylsulfonates constitute an interesting group of substrates or competitors to UCP because of their resemblance to fatty acids but with a pKa for the sulfonic group being much lower than that of the carboxylate. Long-chain alkylsulfonates have been considered as fundamental proofs of the fatty acid cycling mechanism. However, since the pKa of the sulfonic group is too acidic, it cannot be protonated at physiological pH and therefore it cannot flip-flop to allow the transbilayer movement of the proton. This is supported by findings for the first time in respiring BAT mitochondria, concerning the activation of respiration by undecanesulfonate (UDS) E.Rail *et al* (2004).

The results of competition with alkylsulfonates on UCP2 bound to spin-labelled fatty acid have a clear interpretation. If alkylsulfonate is unable to flip-flop and it can activate respiration in a nucleotide-sensitive manner, then the protonophoric cycle cannot be the underlying mechanism of the uncoupling mediated by UCP2. There is another hypothetical mechanism, the “proton buffering model” that proposes that the fatty acid acts as prosthetic group. The carboxylate would bind protons and deliver them to a site from which they are translocated to the other side of the membrane. Alkylsulfonates and fatty acids would provide a group that would be part of the translocation pathway. Although the pKa of an acid group can change significantly depending on the protein environment, it is possible that the pKa of the sulfonic group may be too low to be readily protonable at physiological pH. If this were to be the case, these anionic molecules could act by altering the carrier conformation and transport properties so that protons could overcome the nucleotide inhibition. None of these two possibilities can be dismissed at present. Our results confirm the existence of a binding site for fatty acids on UCP and show that this binding site is identical, at least with a part of the anion channel. The strong evidence for this is provided by the competition of known UCP substrates. Since fatty acids were reported to inhibit alkylsulfonate uniport, the competition of alkylsulfonates and fatty acids is mutual. All our data give further support to the earlier evaluation of the transport mechanism of UCP.

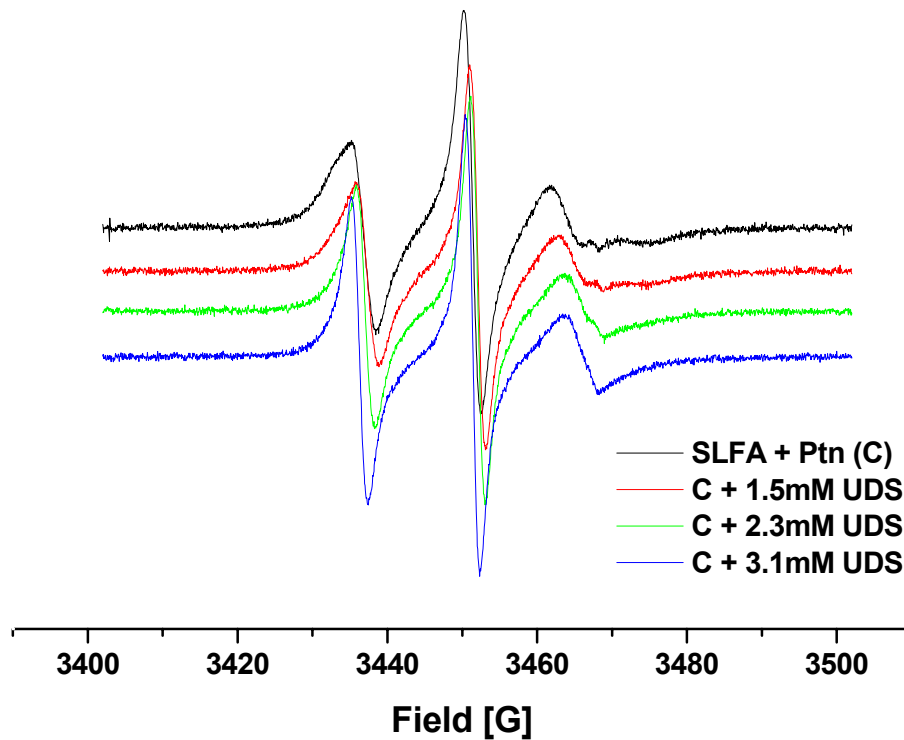


**Fig 3.8:** Competition of undecane sulfonate with UCP2 bound to 7DSA

Electrophoretic proton flux is the *sine qua non* of an uncoupling function. Our data gives evidence to agree with this primary criterion, thereby establishing them as uncoupling proteins in function as well as name. Indeed, the transport properties of UCP2 are qualitatively identical with those of UCP1 with respect to transport of protons and alkylsulfonates. The finding that fatty acids are obligatory for proton flux mediated by UCP2, just as they are for UCP1 has important implications for the biophysical transport mechanism of uncoupling proteins, an issue that is not entirely resolved.

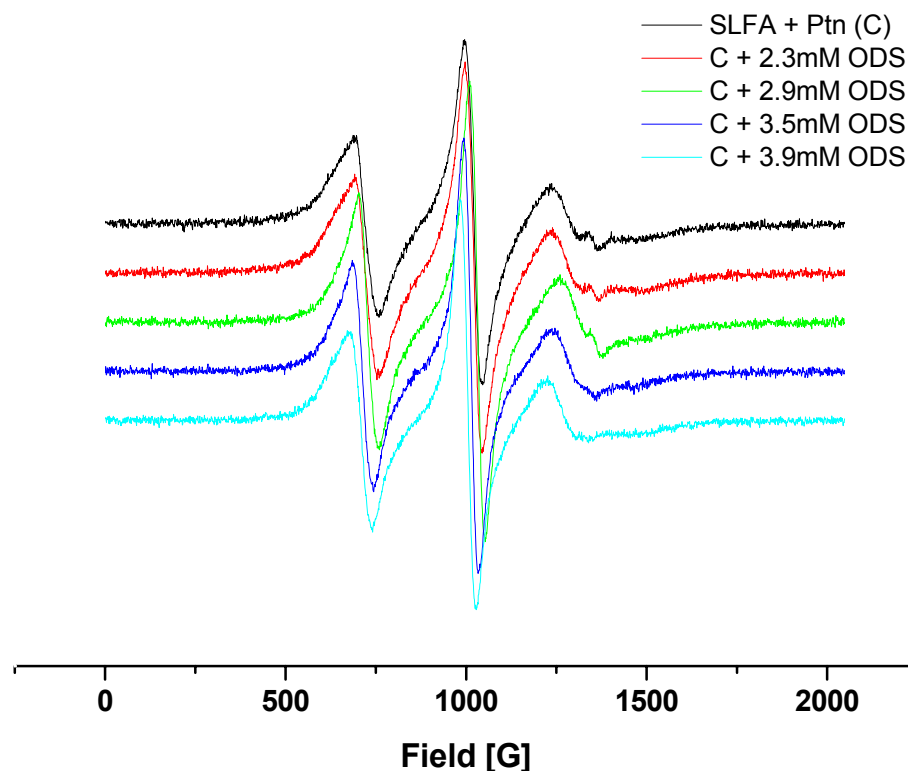


**Fig 3.9:** *Competition of octadecane sulfonate with UCP2 bound to 7DSA*

We favour the fatty acid protonophore model, shown in Fig:1.2, according to which uncoupling proteins contain a transport pathway for the anionic head groups of fatty acid and also probably for alkylsulfonates. The head group is driven from one membrane leaflet to the other by the electric field generated by electron transport. When the fatty acid carboxylate reaches one side, it picks up a proton and rapidly flip-flops back to release the proton to the outer side. The uncoupling proteins thus catalyze a protonophoretic cycle, leading to uncoupling of oxidative phosphorylation.

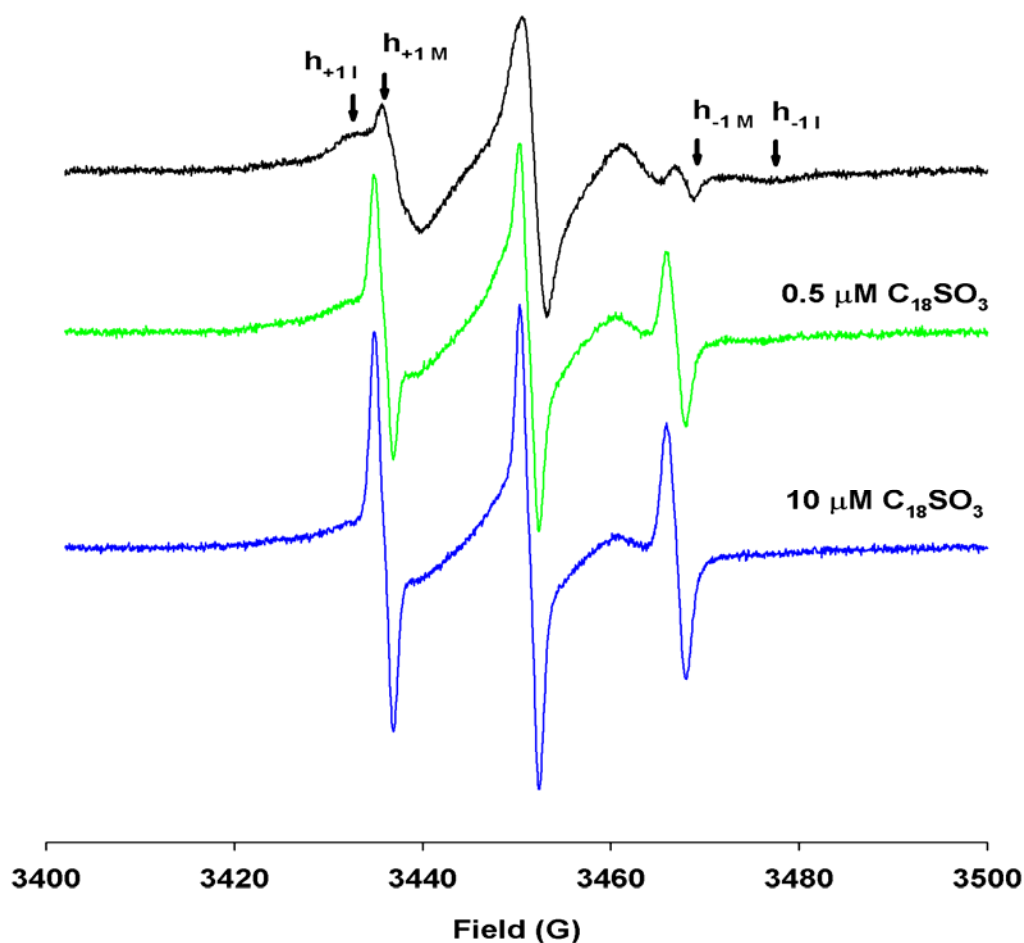


**Fig 3.10:** Competition of octadecane sulfonate with 4PPA bound to UCP2.

An alternative model by Klingenberg and co-workers proposes that UCP1 transports protons, that the transport pathway contains histidines, and that fatty acids function as nonstoichiometric cofactors to buffer intrachannel protons. In a major advance, Bienengraeber *et al.*(1998) demonstrated that substitution of two histidines (H145Q, H147N) in UCP1 caused selective loss of  $H^+$  transport and concluded that these histidines constitute part of the proton conducting pathway. The authors go on to predict that UCP2, which contains neither histidine, will not conduct protons and that UCP3, which contains only one histidine will conduct protons only weakly. In our view, the mutagenesis results are equally consistent with the fatty acid protonophore model and suggest that the histidines in UCP1 form part of the binding site in the fatty acid anion transport pathway. UCP2 and UCP3 possess ample basic residues in this region to fulfil such role (Ježek *et al.* 1998). Our interpretation therefore

predicts that UCP2 and UCP3 will catalyze fatty acid dependent proton transport, and our results with UCP2 thus provide independent support for the postulated fatty acid protonophore model.

Transport of the head group alkylsulfonates also supports the fatty acid protonophore model. In the present study the competition with undecanesulfonate and octadecanesulfonate which are close analogues to laurate and arachidate. Undecanesulfonate is known as competitive inhibitor of laurate induced  $H^+$  transport in UCP1. The sulfonate group is transported across the membrane by both the uncoupling proteins 1 and 2; however, alkylsulfonates do not support  $H^+$  transport. Thus, alkylsulfonates share the anion transport pathway in uncoupling protein with fatty acid, but they cannot complete the protonophoretic cycle. The reason for this failure already discussed in the present chapter being that sulfonates are strong acids and, consequently, cannot deliver protons by electroneutral flip-flop across the bilayer. The fact that the anionic head group of alkylsulfonates is transported across the membrane is a serious problem for the buffering model, because there is no known physicochemical mechanism that would permit alkylsulfonate anion transport and prohibit/inhibit fatty acid anion transport.

### **Role of UCP2 in down-regulation of reactive oxygen species production -**

Any slight increase of the  $H^+$  back flux (to the matrix), which diminishes proton motive force ( $\Delta p$ ), results in a substantial decrease of mitochondrial ROS formation. It can be explained on the basis of increased respiration due to the respiratory control. Slightly increased respiration shortens lifetime of ubisemiquinone radical ( $UQ\cdot$ ) and leads to lowered oxygen tension in the micro environment. Both processes cause reduced rate of  $O_2^{\cdot-}$  formation. Naturally such an increased  $H^+$  backflow proceeds via the  $F_o$  part of ATP-synthase. Hence also during the transition between state 4 (non-phosphorylating resting respiration) to state 3 (ATP synthesis) ROS formation is drastically reduced. In other words, most of ROS are produced *in vivo* under the non-phosphorylating “resting” state. The  $H^+$  backflow given by uncoupling (i.e. by leak or protein-mediated uncoupling) accordingly also decreased the rate of ROS formation rate. Consequently, even the mild uncoupling given by UCP2 (or UCP3 to UCP5), when activated by fatty acids and by releasing purine nucleotide inhibition, can intensively down-regulate ROS production (Nègre-Salvayre *et al.* 1997, Arsenijevic *et al.* 2000).

Downregulation of mitochondrial reactive oxygen species (ROS) production seems to be the most plausible role for UCP2, since its expression is expected in numerous mammal tissues, yet in minute amounts though. The same considerations are valid for UCP3 in skeletal muscle and UCP4 and UCP5 in the brain. Thus the report of Nègre-Salvayre *et al.* could be interpreted as suppression of ROS production due to the UCP2 function. They observed an increased H<sub>2</sub>O<sub>2</sub> production due to membrane potential ( $\Delta\psi$ ) increase induced by GDP addition, likely mediated by UCP2 in macrophage (liver Kupffer cell) mitochondria or in thymus and spleen mitochondria. Also, the UCP2(-/-) and UCP3(-/-) mice exhibited higher levels of ROS in macrophages and muscle, respectively.

Moreover, Brand's group (Echtay et al. 2002) promoted the idea that superoxide itself activates UCP2 by unspecified mechanism from the matrix side. Recently, they rather ascribed such ability to the end-product of the lipoperoxidation cascade for  $\omega$ -6 polyunsaturated fatty acids (PUFAs), to 4-hydroxy-2-nonenal. In addition, Skulachev and Goglia (2003) speculated that fatty acid hydroperoxides can be anionic transport substrates of UCPs, but predicted that they cannot diffuse through the membrane in a protonated form. This speculation was indeed true and proved by our studies with the inability of competition by the added 12-hydroxy-lauric acid (HLA) and 4-hydroxy-2-nonenal (HNE) even at concentrations much higher than the spin label fatty acid. Activation of UCP2 mediated uncoupling by fatty acid hydroperoxides could provide a feedback control mechanism by which the lipoperoxidation product and hence also the product of the increased ROS production activate uncoupling. Thus, this leads to the suppression of ROS production. Similarly, the activation of UCP2 by superoxide proposed by Brand's group could be in fact activation by lipoperoxidation products such as fatty acid hydroperoxides and hydroxy fatty acids, formed downstream in the ROS propagation cascade.

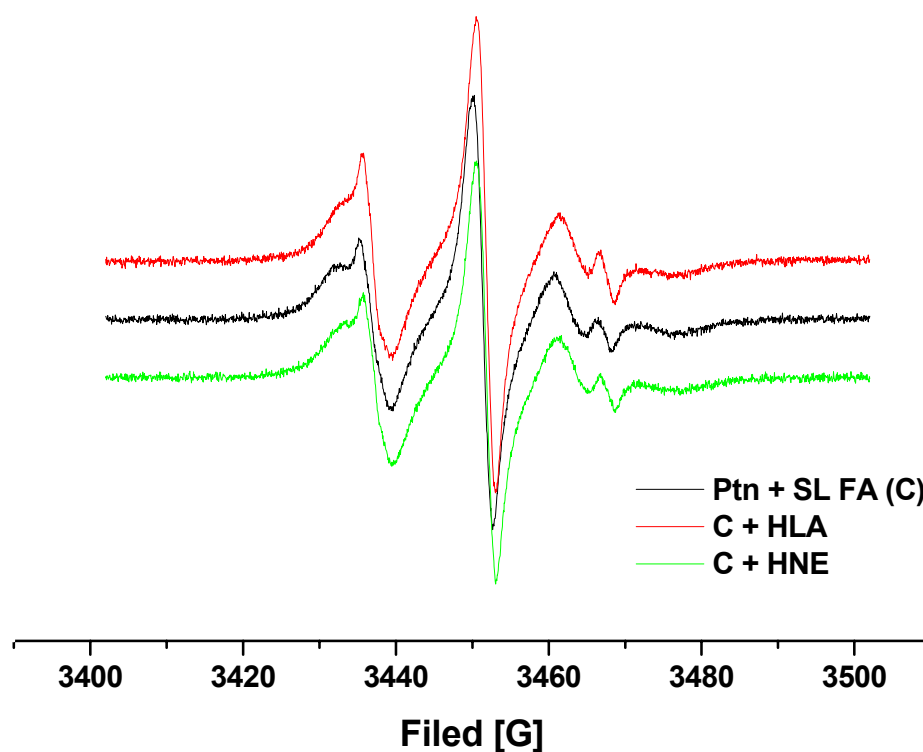


**Fig 3.11:** Illustrates the inactivity of hydroxy fatty acids to displace the bound 4-PPA(112 $\mu$ M) to UCP2(28 $\mu$ M) (HLA: 12-hydroxy lauric acid, HNE: 4-hydroxy -2-nonenal.)

### Effect of purine nucleotides on spin-labelled fatty acid binding to the UCP –

Addition of the native ligand ATP to the spin-labelled fatty acid bound to UCP2 strongly affected this complex which can be clearly seen in the EPR spectra. The changes in the EPR spectra with increasing ATP concentrations were less complicated than those described earlier for alkyl sulfonates and fatty acids. With increasing nucleotide amounts the  $h_{+1i}$  peak decreased and gradually smoothed into a single narrow peak. Alkaline pH, which is known to reduce nucleotide binding as demonstrated by Klingenberg, reversed this effect of ATP on spin label binding in such a way that the original bound spectrum reappeared. UCP2 labelled with spin-labelled fatty acid was inhibited upon addition of ATP of particular concentration with pH 7.0, and at alkaline pH the spectra changed back to the “bound” original form.

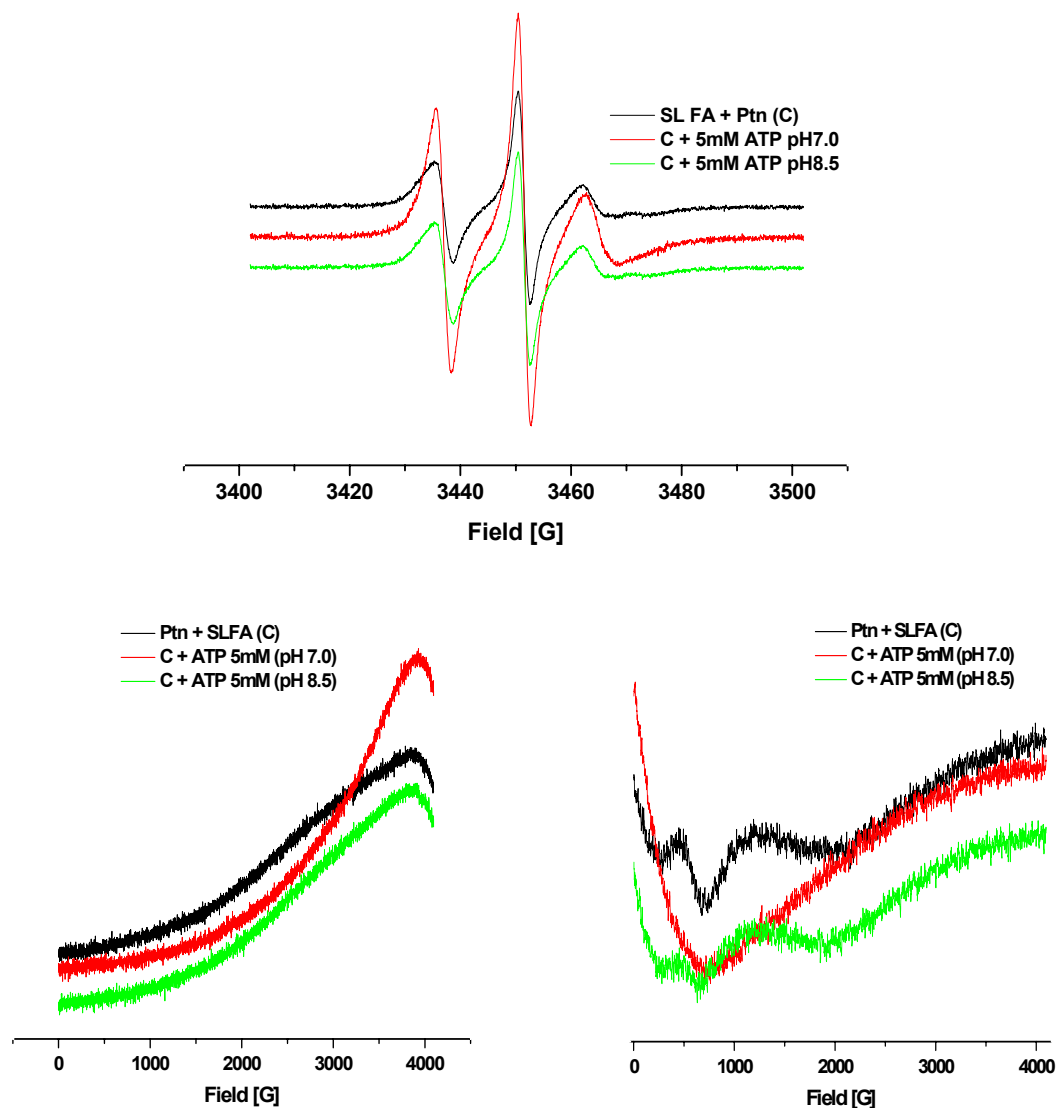


**Fig 3.12:** a) (-) Illustrates ESR spectra of  $100\mu\text{M}$  7-DSA bound to  $24\mu\text{M}$  UCP2, (-) upon addition of  $5\text{mM}$  ATP at neutral pH, (-) upon increasing it to alkaline pH. b) The same titration as above but depicts the clear spectral-shape changes in the low and high-field region.

However we now demonstrate that the spectral changes rather indicate a loss of binding. Under conditions when ATP binding is weak, i.e. at alkaline pH, the spectral changes are reversed to the original bound spectrum. Certain spin-labelled fatty acids embedded in short chain phospholipids and with the nitroxyl group closer to the terminal methyl group

have been reported to give similar spectral changes i.e. larger  $2A_{zz}$  values at high pH. Protonation of the carboxyl group here leads to deeper insertion into the membrane, and deprotonation reverses this effect. In our system of a long chain detergent, such an effect should not occur as proven by experiments in the absence of protein. Hence we conclude that ATP causes partial displacement of bound spin-label from UCP and the probe rebinds at alkaline pH which releases ATP.

Since the influence between ATP and fatty acid is unidirectional, and GDP is a non-competitive inhibitor of anion transport by UCP, we can conclude that the displacement of spin-labelled fatty acid by ATP is allosteric. This displacement mimics the inherent molecular mechanism of gating. Probably, conformational changes switched by ATP prevent exposure of those residues which are essential for binding of anionic substrates. They cause the inaccessibility of the internal anion binding site for anions. The existence of the internal binding site has been suggested previously because of the lack of an external binding site for substrates of UCP, the increasing affinity of more hydrophobic substrates to UCP, and the two-energy barrier profile derived from the flux voltage characteristics.

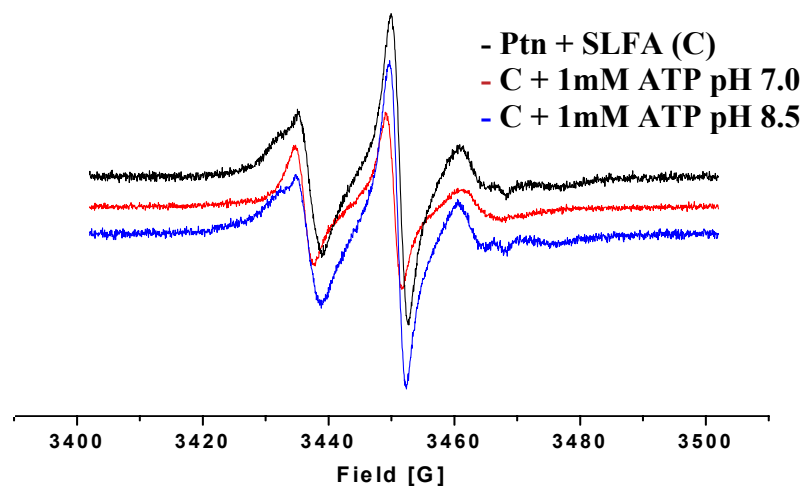


**Fig 3.13:** Illustrates the effect of ATP alkaline pH on 4-PPA bound to UCP2

Inhibition by purine nucleotides is also an essential property of UCP1. Since fatty acids have no effect on the  $K_i$  for nucleotide inhibition, it is generally agreed that transport and inhibition take place on different domains. The nucleotide binding domain in UCP1 is extensive and reasonably well characterized. The sugar base moiety binds to three residues located on the peptide segment that connects helices 5 and 6, an interaction that may confer

selectivity among nucleotides. A glutamate (Glu190) in the fourth transmembrane helix is the pH sensor for nucleotide binding. Three arginines, located in the helices 2, 4, and 6, are required for nucleotide mediated inhibition and have been shown to bind nucleoside phosphates (Modrianský, M *et al.* 1997). Site-directed mutagenesis studies have led to a three-stage binding conformational change model for nucleotide binding and inhibition in UCP1.

It is noteworthy that the seven residues involved in nucleotide mediated inhibition are largely conserved in UCP2, suggesting not only that these proteins would be regulated by nucleotides but also that regulation would be similar among the UCPs. Surprisingly, there are striking differences in nucleotide sensitivity among the UCPs, with UCP2 and UCP3 being only weakly sensitive to GDP, for example. The physiological significance of variations in nucleotide inhibition is unclear, because it is not known how any of the UCPs are opened *in vivo*. In the case of UCP1, a common view is that uncoupling is initiated by dissociation of ATP. In our view, nucleotide debinding is an unlikely opening mechanism: to regulate important physiological processes, nature normally relies on specific signalling pathways and not on the law of mass action. Regulation may involve post-translational modification of the proteins; however, no such signalling pathway has yet been demonstrated in the opening of any of the UCPs.

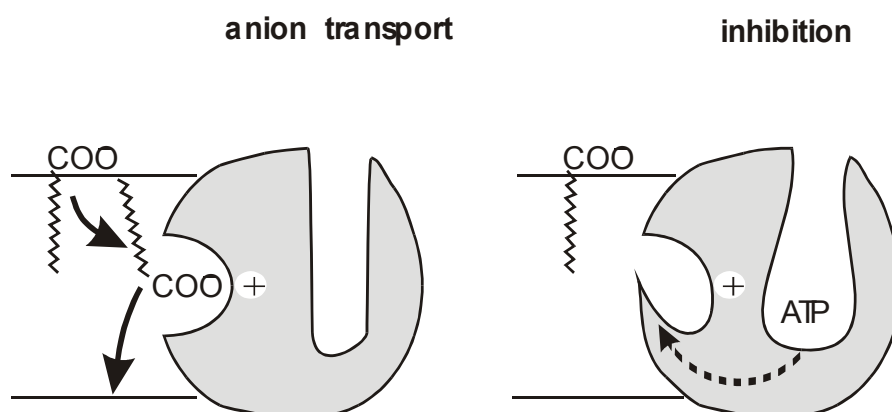


**Fig 3.14:** Model for the molecular mechanism of gating by nucleotides in UCP.

A major value of studies such as these on isolated, reconstituted UCP2 is that this permits direct comparison with similar studies obtained using UCP1. In this regard, our most noteworthy finding is that both the mammalian UCPs are qualitatively identical in mediating fatty acid dependent proton transport. This gives a conclusion and suggestion on future approach, or studies on whole cells and isolated mitochondria containing native UCP are

urgently needed to advance the field. It is hoped that the biophysical approach described here will prove as a useful guide to study on the native system.

## SUMMARY

Uncoupling protein1 (UCP1) in brown adipose tissue was discovered earlier as the main uncoupling source of respiration. We describe the basic facts and a modest contribution of our group to the area of research on mitochondrial uncoupling proteins. After defining the terms uncoupling, leak, proton-mediated uncoupling, we discuss the assumption that due to its low abundance, uncoupling protein 2 (UCP2) can provide only mild uncoupling, i.e. can decrease the proton motive force by several mV only. A fatty acid cycling mechanism is described as a plausible explanation for the protonophoretic function of all uncoupling proteins together with our experiments supporting it. A speculation for the phylogenesis of all uncoupling proteins can be deduced by estimated UCP2 content in several tissues, and details of its activation are explained on the basis of our experiments. In the present study a solubilization and refolding method for UCP2 from inclusion bodies was developed and characterized. As it was known and also demonstrated from previous experiments on UCP1 that fatty acids are substrates, we used the same procedure to study the function of UCP2. Utilizing spin-labelled fatty acids (SLFA) for our experiments we demonstrated the binding of fatty acids to UCP2, and the competition of other natural fatty acids like oleic acid, palmitic acid, arachidonic acid and eicosatrienoic acid to the preformed complex emphasizes the presence of a fatty acid binding site for mitochondrial UCP2. The findings were observed by EPR spectroscopy where the highly immobilized spectra with presence of spin-labelled fatty acid eventually end up as free spin label spectra with a particular concentration of the natural fatty acid added to the UCP2 bound with spin-labelled fatty acid. This fits in significantly with the earlier findings of UCP1 and also leads to assumption of functional explanation about the physiological relevance between the uncoupling proteins functions. The present study, in which representative and sensitive parameters for EPR spectroscopy were established, at the same time describes the concentration effects of fatty acids upon the protein bound with spin-labelled fatty acids which are much of importance in comparison to physiological levels, being in the micromolar range ( $\mu\text{M}$ ) as compared with milli molar (mM) as for UCP1 previously.

In appropriate examples, different fatty acids are used and compared with competitors like alkylsulfonates also emphasizing the function of the protein. And the studies with the effect of nucleotides inhibition demonstrate that there exists a putative binding site for fatty

acids. Much significance lies in demonstration with the spin-labelled-ATP studies where competition of ATP to the protein bound to spin-labelled ATP explains about the inhibition effect of nucleotides on the UCP2. So the present study applies different methods for the functional characterization of UCP2. The studies of natural fatty acids and alkylsulfonates with UCP2 bound to spin-labelled fatty acid, and study of nucleotide inhibition on UCP2 are closely related and give the much awaited answer to the question of functional similarities between UCP1 and UCP2. This supports the discussion of many groups which predict the functional similarity between these two proteins based upon sequence homology. Also many attempts have been reported in literature to explain the physiological functional relevance where by this present study can also be added to as we now suppose from the present conclusions of our experiments.

## ZUSAMMENFASSUNG

Entkoppler-Protein 1 (*uncoupling protein 1*, UCP1) wurde bereits früher als Hauptursache der Atmungs-Entkopplung in braunem Fettgewebe entdeckt. Wir beschreiben hier die grundlegenden Tatsachen sowie unseren Beitrag zur Erforschung der mitochondrialen Entkoppler-Proteine. Nach einer Definition der Begriffe Entkopplung, Leck (*leak*) und Protonen-vermittelte Entkopplung, diskutieren wir die Annahme, dass Entkoppler-Protein 2 (UCP2) auf Grund seines geringeren Vorkommens nur schwache entkoppelnde Wirkung zeigen, d. h. die protonmotorische Kraft nur um wenige mV senken kann. Ein Fettsäure-Austausch-Mechanismus wird als plausible Erklärung für die Protonentransport-Funktion aller Entkoppler-Proteine beschrieben, der durch unsere Ergebnisse unterstützt wird. Eine Spekulation über die Phylogenie aller Entkoppler-Proteine kann durch Abschätzung des UCP2-Gehalts in verschiedenen Geweben abgeleitet werden, und Einzelheiten der Aktivierung können auf Grund unserer Experimente erklärt werden. In der vorliegenden Arbeit wurde eine Solubilisierungs- und Rückfaltungsmethode für UCP2 aus *inclusion bodies* entwickelt und charakterisiert. Da aus früheren Experimenten mit UCP1 bekannt war, dass Fettsäuren als Substrate fungieren, benutzten wir beim Studium der Funktion von UCP2 dieselbe Vorgehensweise wie dort. Unter Verwendung von spinmarkierten (*spin-label*-, SL-)Fettsäuren für unsere Experimente demonstrierten wir die Bindung von Fettsäuren an UCP2, und die Konkurrenzreaktion natürlicher Fettsäuren wie Ölsäure, Palmitinsäure, Arachidonsäure und Icosatriensäure am vorgeformten Komplex unterstreicht das Vorhandensein einer Fettsäure-Bindungstasche bei mitochondrialem UCP2. Die Beobachtungen wurden mit Hilfe von EPR-Spektroskopie gemacht, wobei zunächst bei Zugabe von SL-Fettsäure zu UCP2 Spektren erhalten werden, die für hohe Immobilisierung typisch sind, die aber bei Zugabe bestimmter Konzentrationen natürlicher Fettsäuren in die Spektren der freien SL-Fettsäure übergehen. Dies passt bedeutsamerweise zu den früheren Ergebnissen mit UCP1 und führt auch zu einer Annahme über die physiologische Relevanz der Funktionen der Entkoppler-Proteine. Die vorliegende Studie, in der repräsentative und sinnvolle Parameter für die EPR-Spektroskopie erarbeitet wurden, beschreibt zugleich Konzentrationseffekte von Fettsäuren auf den Komplex von Protein und SL-Fettsäure, die auch im Hinblick auf physiologische Konzentrationen durchaus Bedeutung haben, da sie im mikromolaren Bereich auftreten im Gegensatz zum millimolaren zuvor bei UCP1.

Eine geeignete Auswahl verschiedener Fettsäuren wurde als Kompetitoren benutzt und in dieser Eigenschaft mit Alkylsulfonaten verglichen, wodurch ebenfalls die Funktion des Proteins deutlich gemacht wurde. Untersuchungen des Effekts der Inhibierung durch Nucleotide zeigen ebenfalls die Existenz der fraglichen Fettsäure-Bindungstasche. Große Bedeutung liegt in der Demonstration der Verdrängung von SL-ATP durch ATP aus dem Komplex mit dem Protein, wodurch der inhibitorische Effekt von Nucleotiden auf UCP2 erklärt wird. Hierzu werden in der vorliegenden Arbeit verschiedene Methoden zur funktionellen Charakterisierung von UCP1 angewandt. Die Untersuchungen natürlicher Fettsäuren und Alkylsulfonate mit UCP2 im Komplex mit spinmarkierter Fettsäure und die Untersuchung der Nucleotid-Inhibition von UCP2 hängen eng zusammen und geben die lang erwartete Antwort auf die Frage nach funktionellen Ähnlichkeiten bei UCP1 und UCP2. Dies stellt die Diskussionen vieler Gruppen auf eine neue Grundlage, die die funktionelle Ähnlichkeit beider Proteine auf Basis der Sequenzhomologie vorhersagen. Es gab auch viele Versuche in der Literatur, die physiologische Relevanz aufzuklären, wozu durch diese Untersuchungen, nach unseren gegenwärtigen Experimenten zu schließen, ebenfalls ein Beitrag geleistet werden kann.

**REFERENCES**

Arechaga, I., Raimbault, S., Prieto, S., Levi-Meyrueis, C., Zaragoza, P., Miroux, B., Ricquier, D., Bouillaud, F. & Rial, E. (1993) Cysteine residues are not essential for uncoupling protein function. *Biochem. J.* **296**, 693-700.

Arsenijevic, D., Onuma, H., Pecqueur, C., Raimbault, S., Manning, B.S., Couplan, E., Alves-Guerra, M.C., Goubern, M., Surwit, R., Ricquier, D. (2000) Disruption of the uncoupling protein 2 gene in mice reveals a role in immunity and reactive oxygen species production. *Nat Genet.* **26**, 435-439.

Aquila, H., link, T.A., and Klingenberg, M. (1985) *EMBO J.* **4**, 2369-2376.

Auchampach, J.A., Grover, G.J., and Gross, G.J., (1992) *Cardiovasc. Res.* **26**, 1054-1062.

Akerman, K.E., and Wikstrom, M.K. (1976) Safranin as a probe of the mitochondrial membrane potential. *FEBS Lett.* **68**, 191-197.

Antunes, F., Salvador, A., Marinho, H.S., Alves, R., Pinto, R.E., (1996) Lipid peroxidation in mitochondrial inner membranes I. An integrative kinetic model. *Free Radic. Biol. Med.* **21**, 917-943.

Azzi, A., Montecucco, C., Richter, C., (1975) The use of acetylated ferricytochrome c for the detection of superoxide radicals produced in biological membranes. *Biochem. Biophys. Res. Commun.* **65**, 597-603.

Barja, G., (2004) Aging in vertebrates, and the effects of caloric restriction: a mitochondrial free radical production-DNA damage mechanism? *Biol. Rev. Camb. Philos. Soc.* **79**, 235-251.

Barja, G., Herrero, A. (2000) Oxidative damage to mitochondrial DNA is inversely related to maximum life span in the heart and brain of mammals. *FASEB J.* **14**, 312-318.

Beal, M.F. (2003) Mitochondria, oxidative damage, and inflammation in Parkinson's disease. *Ann. N.Y. Acad. Sci.* **991**, 120-131.

Beckman, J.S., Beckman, T.W., Chen, J., Marshall, P.A., Freeman, B.A., (1990) Apparent hydroxyl radical production by peroxynitrite: implications for endothelial injury from nitric oxide and superoxide. *PNAS U.S.A.* **87**, 1620-1624.

Bedogni, B., Pani, G., Colavitti, R., Riccio, A., Borrello, S., Murphy, M., Smith, R., Eboli, M.L., Galeotti, T. (2003) Redox regulation of cAMP-responsive element-binding protein and induction of manganese superoxide dismutase in nerve growth factor-dependent cell survival. *J. Biol. Chem.* **278**, 16510-16519.

Bezaire, V., Hofmann, W.E., Kramer, J.K.G., Kozak, L.P., and Harper, M.E. (2001) Effects of fasting on muscle mitochondrial energetics and fatty acids metabolism in Ucp3<sup>-/-</sup> and wild type mice. *Am. J. Physiol.* **281**: E975-E982.

Blaxter, K.L. (1989) The minimal metabolism: Energy metabolism in Animals and Man. *C.U.Press. Cambridge, U.K.* **pg:** 120-146.

Boss, O., Hagen, T., and Lowell, B.B. (2000) Uncoupling proteins 2 and 3: potential regulators of mitochondrial energy metabolism. *Diabetes.* **49**, 143-156.

Brand, M.D. (1990) The contribution of the leak of protons across the mitochondrial inner membrane to standard metabolic rate. *J. Theor. Biol.* **145**, 267-286.

Brand, M.D. (2000) Uncoupling to survive? The role of mitochondrial inefficiency in ageing. *Exp. Gerontol.* **35**, 811-820.

Brand, M.D., Steverding, D., Kadenbach, B., Stevenson, P.M., and Hafner, R.P. (1992) The mechanism of the increase in mitochondrial proton permeability induced by thyroid hormones. *Eur. J. Biochem.* **206**, 775-781.

Brand, M.D., Chein, L.F., Ainscow, E.K., Rolfe, D.F.S., and Porter, R.K. (1994) The causes and functions of mitochondrial proton leak. *Biochim. Biophys. Acta.* **1187**, 132-139.

- Brand, M.D., Brindle, K.M., Buckingham, J.A., Harper, J.A., Rolfe, D.F.S., and Stuart, J.A. (1999) The significance and mechanism of mitochondrial proton conductance. *Int. J. Obes. Relat. Metab. Disord.* **23**, (Suppl 6): S4-S11.
- Brown, G.C., Lakin-Thomas, P.L., and Brand, M.D. (1990) Control of mitochondrial respiration and ATP synthesis in isolated rat liver cells. *Eur. J. Biochem.* **192**, 355-362.
- Burns, R.J., Smith, R.A., Murphy, M.P. (1997) Labelling of mitochondrial proteins in living cells by the thiol probe thiobutyltriphenylphosphonium bromide. *Arch. Biochem. Biophys.* **339**, 33-39.
- Burns, R.J., Smith, R.A., Murphy, M.P. (1995) Synthesis and characterization of thiobutyltriphenylphosphonium bromide, a novel thiol reagent targeted to the mitochondrial matrix. *Arch. Biochem. Biophys.* **322**, 60-68.
- Buttgereit, F., and Brand, M.D. (1995) A hierarchy of ATP-consuming processes in mammalian cells. *Biochem. J.* **312**, 163-167.
- Casteilla, L., Champigny, O., Bouillaud, F., Robelin, J., and Ricquier, D. (1989) Sequential changes in the expression of mitochondrial protein mRNA during the development of brown adipose tissue in bovine and ovine species. *Biochem. J.* **257**, 665-671.
- Casteilla, L., Forest, C., Robelin, J., Ricquier, D., Lombet, A., and Aillaud, G. (1987) Characterization of mitochondrial uncoupling protein in bovine fetus and newborn calf. *Am. J. Physiol.* **252**, 627-636.
- Challoner, D.R. (1968) Respiration in myocardium. *Nature (Lond)* **217**, 78-79.
- Clausen, T., van Hardeveld, C., and Everts, M.E. (1991) Significance of cation transport in control of energy metabolism, and thermogenesis. *Physiol. Rev.* **71**, 733-774.
- Enerback, S., Jacobsson, A., Simpson, E.M., Guerra, C., Yamashita, H., Harper, M.E., and Kozak, L.P. (1997) Mice lacking mitochondrial uncoupling protein are cold sensitive but not obese. *Nature (Lond)* **387**, 90-94.

- Fleury, C., Neverova, M., Collins, S., Raimbault, S., Champigny, O., Levi-Meyrueis, C., Bouillaud, F., Seldin, M.F., Surwit, R.S., Ricquier, D., and Warden, C.H. (1997) Uncoupling protein-2: A novel gene linked to obesity and hyperinsulinemia. *Nat. Genet.* **15**, 269-272.
- Garlid, K.D., Orosz, D.E., Modrianský, M., Vassanelli, S., Ježek, P. (1996) On the mechanism of fatty acid-induced proton transport by mitochondrial uncoupling protein. *J. Biol. Chem.* **271**, 2615-2620.
- Garlid, K.D., Jabůrek, M., Ježek, P. (1998) The mechanism of proton transport mediated by mitochondrial uncoupling proteins. *FEBS Lett.* **438**, 10-14.
- Garlid, K.D., Jabůrek, M., Ježek, P., Vařecha, M., (2000) How do uncoupling proteins uncouple? *Biochim. Biophys. Acta.* **1459**, 383-389.
- Garlid, K.D., Jabůrek, M., Ježek, P. (2001) Mechanism of uncoupling protein action. *Biochem Soc Trans.* **276**, 803-806.
- Hanák, P., Ježek, P. (2001) Mitochondrial uncoupling proteins and phylogenesis – UCP4 as the ancestral uncoupling protein. *FEBS Lett.* **495**, 137-141.
- Hide, E.J. and Thiemermann, C. (1996) *Cardiovasc. Res.* **26**, 1054-1062.
- Jabůrek, M., Garlid, K.D. (2003) Reconstitution of recombinant uncoupling proteins: UCP1, 2, and 3, have similar affinities for ATP and are unaffected by coenzyme Q10. *J. Biol. Chem.* **278**, 25825-25831.
- Jabůrek, M., Vařecha, M., Ježek, P., Garlid, K.D. (2001) Alkylsulfonates as probes of uncoupling transport mechanism. Ion pair transport demonstrates that direct H<sup>+</sup> translocation by UCP1 is not necessary for uncoupling. *J. Biol. Chem.* **276**, 31897-31905.
- Jabůrek, M., Vařecha, M., Gimeno, R.E., Dembski, M., Ježek, P., Garlid, K.D. (1999) Transport function and regulation of mitochondrial uncoupling proteins 2 and 3. *J. Biol. Chem.* **274**, 26003-26007.

Ježek, P. (1999) Fatty acid interaction with mitochondrial uncoupling proteins. *J Bioenerg Biomemb.* **31**, 457-466.

Ježek, P. (2002) Possible physiological roles of mitochondrial uncoupling proteins – UCPn. *Int. J Biochem Cell Biol.* **34**, 1190-1206.

Ježek, P., Freisleben, H-J. (1994) Fatty acid binding site of the mitochondrial uncoupling protein. Demonstration of its existence by EPR spectroscopy of 5-DOXYL-stearic acid. *FEBS Lett.* **343**, 22-26.

Ježek, P. Garlid, K.D. (1990) New substrates and competitive inhibitors of the  $\text{Cl}^-$  translocating pathway of the uncoupling protein of brown adipose tissue mitochondria. *J. Biol. Chem.* **265**, 19303-19311.

Ježek, P. Garlid, K.D. (1998) mammalian mitochondrial uncoupling proteins. *Int J Biochem Cell Biol.* **30**, 1163-1168.

Ježek, P. Ježek, J. (2003) Sequence anatomy of mitochondrial anion carriers. *FEBS Lett.* **534**, 15-25.

Ježek, P., Orosz, D.E., Modrianský, M., Garlid, K.D. (1994) Transport of anions and protons by the mitochondrial uncoupling protein and its regulation by nucleotides and fatty acids: a new look at old hypotheses. *J. Biol. Chem.* **269**, 26184- 26190.

Ježek, P., Bauer, M., Trommer, W.E. (1995) EPR spectroscopy of 5-DOXYL-stearic acid bound to the mitochondrial uncoupling protein reveals its competitive displacement by alkylsulfonates in the channel and allosteric displacement by ATP. *FEBS Lett.* **361**, 303-307.

Ježek, P., Modrianský, M., Garlid, K.D. (1997) Inactive fatty acids are unable to flip-flop across the lipid bilayer. *FEBS Lett.* **408**, 161-165.

Ježek, P., Modrianský, M., Garlid, K.D. (1997) A structure activity study of fatty acid interaction with mitochondrial uncoupling protein. *FEBS Lett.* **408**, 166-170.

- Klingenberg, M. (1990) Mechanism and evolution of the uncoupling protein of brown adipose tissue. *Trends Biochem Sci.* **15**, 108-112.
- Klingenberg, M., Huang, S-G. (1999) Structure and function of the uncoupling protein from brown adipose tissue. *Biochim Biophys Acta.* **1415**, 271-296.
- Klingenberg, M., Winkler, E. (1985) The reconstituted isolated uncoupling protein is a membrane potential driven H<sup>+</sup> translocator. *EMBO J.* **4**, 3087-3092.
- Nicholls, D.G. (1974) Hamster brown adipose tissue mitochondria. *Eur. J. Biochem.* **49**, 573-583.
- Nicholls, D.G., Lindberg, O. (1973) Brown adipose tissue mitochondria. The influence of albumin and nucleotides on passive ion permeabilities. *Eur. J. Biochem.* **37**, 523-530.
- Růžička, M., Borecký, J., Hanuš, J., Ježek, P. (1996) Photoaffinity labelling of the mitochondrial uncoupling protein by [<sup>3</sup>H] azido fatty acid affects the anion channel. *FEBS Lett.* **382**, 239-243.
- Skulachev, V.P. (1991) Fatty acid circuit as a physiological mechanism of uncoupling of oxidative phosphorylation. *FEBS Lett.* **294**, 158-162.
- Skulachev, V.P. (1998) Uncoupling: new approaches to an old problem of bioenergetics. *Biochim Biophys Acta.* **1363**, 100-124.
- Skulachev, V.P., Goglia, A. (2003) *FASEB J.* **17**, 1585-1591.
- Winkler, E., Klingenberg, M. (1994) Effect of fatty acids on H<sup>+</sup> transport activity of the reconstituted uncoupling protein. *J. Biol. Chem.* **269**, 2508-2515.
- Žáčková, M., Ježek, P. (2002) Reconstitution of novel mitochondrial uncoupling proteins UCP2 and UCP3. *Biosci Rep.* **22**, 33-46.

Žáčková, M., Krämer, R., Ježek, P. (2000) Interaction of mitochondrial phosphate carrier with fatty acids and hydrophobic phosphate analogs. *Int J Biochem Cell Biol.* **32**, 499-508.

Suckling, K.E., and Suckling, C.J. (Edition) *Biological Chemistry – The molecular approach to biological synthesis.*

Lehninger, Nelson, and Cox (Edition) *Principles of Biochemistry.*

Lubert Stryer (Edition) *Biochemistry.*

**Curriculum Vitae**

Mandapati V.L. Narasimha Raju

E.C.A. & I.S.Ltd	Erwin Schroedinger Str 54
Etikoppaka	Dept of Chemistry/Biochemistry
531082 – Vizag Dt	67663 – Kaiserslautern
INDIA	GERMANY

Date of Birth	11 <sup>th</sup> August 1977
Place of Birth	Vijaywada/India
Nationality	Indian
1993 – 1995	Senior Secondary School Board, A.P India
1995 – 1998	Bachelor of Science, Andhra University India
1998 – 2000	Master of Science, Andhra University India
2000 – 2001	Junior Research Fellow, I.I.Sc India
2001 – 2003	Research Fellow (CSIR NET), I.I.Sc India
2003 – 2006	Ph.D thesis at Department of Chemistry/Biochemistry, TU Kaiserslautern, Germany. Supervisors: Prof. Wolfgang Trommer and Dr. Petr Ježek, Prague.

## Acknowledgments

First of all, I would like to thank Mr. Wolfgang Trommer for his support and guidance during my thesis. I got his scientific and personal advice anytime I needed it, and for the plenty take home messages he has given me to build and grow my career, last and not the least to the freedom and individuality he gave me for the organization of my thesis work.

My special thanks go to Mr. Petr Ježek for his kind suggestions and discussions and the technical support in his lab. His enthusiasm and energy is only exceeded by his ability to create a joyous working atmosphere.

And my kind thanks to Mr. Reinhard Philipp for spending his time and energy for the corrections of my thesis work and being very prompt for my updatings, and also his great extensive knowledge which he taught me a lot, last but not the least his ever interesting company during all the group casual gatherings.

My thanks go to Mrs. Carolin Fluck for her never ending energy in making all the reasonable and most important office paper work of my contracts and administrative submissions.

And my sincere thanks to one of my dearest friend and colleague Ms. Irene Caminiti, who studied her diploma in this group for her kind discussions and heartfelt kind memorable time which was ever lasting motivation for my work.

I would like to thank best friends Dirk Mannweiler and Martin Hossann for their ever lasting kind and memorable support without whom my work would never be complete, I cherished their kind heartfelt friendship which I had at any given time during my stay.

My Special thanks to Elke Litmianski and Yvonne Lorat for their kind assistance and timely organization of the technical supervision for my work.

I would like to thank one and all of my friends and colleagues in my working group, Stefan Hauck, Anja Baron, Fabian Leinisch, Sabine Becht, Michaela Haimann, and my senior colleagues Olaf Becker, Fabian Roazario, Ralf Berger, Dawin Hyllus and Tassilo Hornung for their kind cooperation and help during my entire period here. And also each and every

colleague in Petr Ježeks group, along with the friends and colleagues in the DFG graduate college.

“Last and not the least” I would also like to convey my sincere respects to Mr. Wolfgang Trommer, Mrs. Jutta Trommer and Ms. Tanya Trommer for their ever lasting kindness and generosity and making my time memorable for keeping me realized of a family away from home. Words could not last for their support and love showered to me.

## Acknowledgments

The experimental work of the present described thesis work was carried out in between the period April 2004 and March 2006, under the supervision of Prof. Wolfgang Trommer, and also few experiments were done in the laboratory of Dr. Petr Ježek, Prague under a collaboration project under the CAS-DAAD programme.

My deepest respect and thanks to Prof. Wolfgang Trommer for giving me a chance to work and expand my knowledge for the present theme of thesis work. His everlasting enthusiasm and discussions gave me great motivation for the successful completion of my work.

Thanks to Dr. Petr Ježek for giving me support and constructive ideas for the present work and his energy in making my work and myself fruitful and creative.